

THE NATURE OF SYMBIOTIC STARS¹

SCOTT J. KENYON AND RONALD F. WEBBINK

Department of Astronomy, University of Illinois at Urbana-Champaign

Received 1982 April 26; accepted 1983 September 2

ABSTRACT

Synthetic spectra from 0.1 to 3.5 μm are computed for various binary models of symbiotic stars. These models consist of three components: (i) a late-type giant or bright giant, (ii) a hot companion, and (iii) a surrounding nebula which is photoionized by the hot component. Hot stellar sources, disk accretion onto white dwarf stars, and disk accretion onto main sequence stars are considered as possible hot components. The model nebular contribution includes the nebular continuum and line radiation from H and He⁺, assuming a nebula optically thick at wavelengths below the ionization edges and case B recombination. Reddening-free ultraviolet (UV) continuum colors are derived for these synthetic spectra, assuming a standard interstellar extinction curve, and are used to construct a diagnostic UV color-color diagram in which the trajectories of hot stellar sources, accreting white dwarfs, and accreting main sequence stars are well separated.

UV continuum colors are estimated for 19 symbiotic and related objects with *IUE* low-resolution spectra available to us, and these are compared to the reddening-free indices derived from the models. Several symbiotic stars are identified as certain or probable main sequence accretors, with mass accretion rates in the range from a few times 10^{-6} to $10^{-4} M_{\odot} \text{ yr}^{-1}$: Z And, CI Cyg, YY Her, AR Pav, and CL Sco. Most of the remaining systems appear to contain hot stellar companions with temperatures in the range $\log T = 4.6$ to 5.1: BF Cyg, AG Dra, V443 Her, RW Hya, SY Mus, and AG Per. Relatively low temperature solutions ($\sim 10^4$ K) are indicated for the symbiotic-like objects TX CVn and *o* Cet B. UV continuum diagnostics are unreliable for systems showing strong circumstellar dust emission (e.g., R Aqr, V1016 Cyg, RX Pup), and a few objects (T CrB, CH Cyg, BX Mon) conform to no models. However, no example could be found of a symbiotic star in which the UV continuum originates from an accretion disk surrounding a white dwarf star. Each of the systems examined is briefly discussed in the light of the model spectra.

The Balmer line fluxes predicted by the models are in good agreement with observations, while the He II $\lambda 4686$ emission is underpredicted by factors of 2-100. Photoionization of He II from the $n = 2$ level can increase the theoretical $\lambda 4686$ flux to the observed value in some systems with dense nebulae (e.g., AG Peg), but this mechanism appears inadequate for other symbiotic stars. Hydromagnetic waves generated in a turbulent boundary layer may provide an additional source of ionization in the nebulae of these systems.

The optical spectrum of a symbiotic star in outburst may be produced by either (i) a blackbody at $T_{\text{eff}} \approx 6000$ -10,000 K, (ii) a white dwarf accreting matter at a rate *above* the Eddington limit ($\dot{M} > 10^{-5} M_{\odot} \text{ yr}^{-1}$), or (iii) a main sequence star accreting matter near the Eddington limit ($\dot{M} \sim 10^{-3} M_{\odot} \text{ yr}^{-1}$). We describe the evolution of the outburst for each of these possibilities, and identify the critical stages when ultraviolet and optical spectra should be obtained.

Subject headings: spectrophotometry — stars: accretion — stars: binaries — stars: combination spectra

I. INTRODUCTION

The symbiotic stars were discovered by Cannon and Merrill to have the absorption features of a late-type giant in combination with a high excitation emission-line spectrum. Infrared photometry has confirmed that a late-type star is present in most symbiotic stars, and usually this is an M-type giant (cf. Allen 1979). The observations of bright emission lines and a veiling blue continuum in these systems are most naturally explained by a binary model in which the high-temperature features are associated with a hot companion to the giant. Recent observations of many symbiotic systems with the *IUE* satellite (Keyes and Plavec 1980; Slovak 1980; Johnson 1980; Michalitsianos, Kafatos, and Hobbs 1980;

Altamore *et al.* 1981; Stencel *et al.* 1982) support this idea: the UV spectra are dominated by strong emission lines (e.g., C IV $\lambda\lambda 1548, 1550$ and He II $\lambda 1640$) superposed on a hot continuum source. For most of these sources, the orbital period, and thus the basic physical parameters of the two components, is unknown. Because of this, the nature of the hot component must be inferred by indirect methods.

Berman (1932) and Hogg (1934) first interpreted the spectra of symbiotic stars in terms of a binary model. Both suggested that a hot, compact star (i.e., far below the main sequence) would provide an excellent source for emission lines, and yet would be nearly invisible in the optical. Later, Kuiper (1940) proposed that accretion onto an otherwise normal main sequence star from a Roche lobe filling companion might explain such peculiar stars as β Lyr and Z And. Recent elaborations of both these models have concentrated upon explaining the outbursting nature of the best-observed

¹ This research was supported by the National Science Foundation through grants AST 80-18198 and AST 80-18859, and by the University of Illinois Research Board.

examples of symbiotic stars (Tutukov and Yungel'son 1976; Bath 1977; Paczyński and Żytkow 1978; Paczyński and Rudak 1980; Bath and Pringle 1982).

Until the near-ultraviolet part of the spectrum became accessible through satellite observations, the most noteworthy observational efforts to determine the physical properties of the hot components in individual systems attempted to explain the optical nebular spectrum in terms of a specific model for the hot stellar companion (e.g., Boyarchuk 1969). The advent of satellite UV observations has led to a broader appreciation among both observers and theoreticians for the complexities of the emission-line systems of symbiotic stars, but it has also for the first time permitted the direct observation of an extended underlying continuum attributable directly to the hot component. Several attempts have been made to fit these continua to stellar atmospheres (Gallagher *et al.* 1979; Keyes and Plavec 1980; Slovak 1980, 1982; Altamore *et al.* 1981; Michalitsianos *et al.* 1982a) with mixed success: certain symbiotic stars (most notably AG Peg; Gallagher *et al.* 1979; Keyes and Plavec 1980) appear to conform closely to this model, whereas others (YY Her, for example; Michalitsianos *et al.* 1982a) would appear to defy such simple explanations. To the best of our knowledge, however, no attempt has been made prior to that described here to explore in detail the viability of accretion disk models for the ultraviolet flux distributions.

Our purpose in this paper is to survey the range of binary models which give rise to identifiably symbiotic optical spectra. The primary objective is to identify the most pronounced observable differences among the various possible models, and then to devise simple, reliable, reddening-free diagnostic tests to permit an *observational* classification of known symbiotic stars according to the nature of their underlying hot components. The main thrust of our study lies in understanding and reproducing the gross features of the continuum flux distributions in symbiotic stars, since apart from a possible nebular contribution, each of the various models of symbiotic stars makes rather specific, inflexible predictions regarding the form of that distribution (at least in the accessible spectral range) with the specification of a minimum number of free parameters. Modeling of the nebular spectrum, on the other hand, introduces a number of additional variables (such as nebular density and electron temperature, filling factor, etc.) including, importantly, knowledge of its excitation mechanism. As we shall see, diagnostic tests do indeed exist which provide a relatively clear distinction among possible models, especially when observations are available throughout the outburst of a symbiotic star. At the same time, our results raise new problems in understanding the nebular emission from many of these systems.

In the discussion that follows, we consider three-component models of symbiotic stars (cf. Boyarchuk 1967) consisting of (i) a late-type giant or bright giant; (ii) a hot component, being either an accretion disk surrounding a low mass companion (white dwarf or main sequence star) to the giant, or a hot, compact star similar to the central star of a planetary nebula; and (iii) a surrounding gaseous nebula ionized by the hot component. The continuous spectrum of the nebula and a given hot component can be calculated in a straightforward manner, and can be combined with observed spectra of selected late-type giants to construct synthetic

spectra over the 1000–35,000 Å range. Our method of calculation is described in the next section, and the model spectra are presented in § III. These models may be used to identify the defining features of various hot components, which are compared with the observed properties of symbiotic stars in §§ IV–VI. The outbursts of symbiotic stars are discussed in § VII. We conclude with a brief summary of our findings.

II. CALCULATION OF THE EMITTED SPECTRUM

a) Spectrum of the Hot Component

The observed spectrum of a hot stellar photosphere can be written as

$$F_h(\lambda, T_h) = (R_h/d)^2 \mathcal{F}_h(\lambda, T_h), \quad (1)$$

where R_h is the radius of the star, d is its distance, and \mathcal{F}_h is the emitted flux at a given wavelength in units of $\text{ergs cm}^{-2} \text{s}^{-1} \text{Å}^{-1}$. We use Kurucz (1979) model atmospheres for hot components having relatively low effective temperatures ($T_h \lesssim 50,000$ K). Although models are available for higher effective temperatures (e.g., Wesemael *et al.* 1980; Wesemael 1981; Hummer and Mihalas 1970), Kaler (1976) has found that a blackbody approximation to the far-UV flux from central stars of planetary nebulae yields a more consistent description of the nebular emission. In the near-UV, model atmospheres converge toward the Rayleigh-Jeans tail of a blackbody at high temperatures ($T_h > 50,000$ K), so it will be assumed that the spectra of these hot components are well approximated by a blackbody.

The spectrum emitted by material accreting onto a star has been analyzed in detail by Shakura and Sunyaev (1973) and Lynden-Bell and Pringle (1974). We assume a steady-state, time-independent accretion disk around a central star of mass M_1 and radius R_1 . If the accretion rate is given by \dot{M} , the temperature as a function of radius R in the disk will be

$$T_d(R) = \left\{ \frac{3GM_1\dot{M}}{8\pi\sigma R^3} \left[1 - \left(\frac{R_1}{R} \right)^{1/2} \right] \right\}^{1/4}, \quad (2)$$

where G is the gravitational constant and σ is the Stefan-Boltzmann constant.

About one-half of the accretion energy ($GM_1\dot{M}/2R_1$) is radiated by the accretion disk itself; the rest must be radiated in a boundary layer near the central star (Lynden-Bell and Pringle 1974). The temperature structure of this region was first examined by Lynden-Bell and Pringle, and then by Pringle (1977) and by Pringle and Savonije (1979). If pressure and the rotational velocity of the central star can be neglected, the temperature may be approximated by (Lynden-Bell and Pringle 1974)

$$T_{\text{BL}} \approx 6.5 \times 10^4 \left(\frac{M_1\dot{M}}{10^{-5} M_\odot^2 \text{yr}^{-1}} \right)^{1/4} \left(\frac{R_1}{R_\odot} \right)^{-3/4}. \quad (3)$$

If gas pressure is important in the boundary layer, this expression is modified to (Pringle 1977):

$$T_{\text{BL}} \approx 4.5 \times 10^4 \left(\frac{\dot{M}}{10^{-5} M_\odot \text{yr}^{-1}} \right)^{2/9} \left(\frac{M_1}{M_\odot} \right)^{1/3} \left(\frac{R_1}{R_\odot} \right)^{-7/9} \text{K}. \quad (4)$$

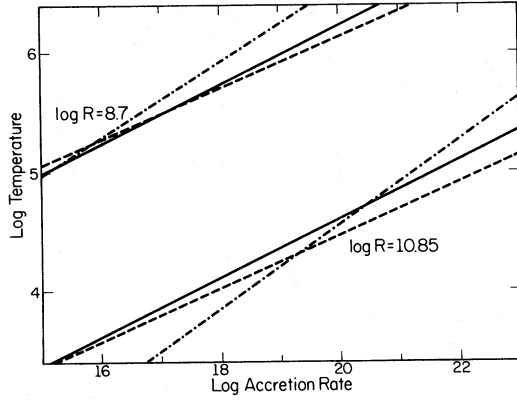


FIG. 1.—Boundary layer temperature as a function of accretion rate for a $1 M_{\odot}$ white dwarf and a $1 M_{\odot}$ main sequence star. The solid line represents the relation derived by Lynden-Bell and Pringle (1974), while the dashed line shows the temperature derived by Pringle (1977). The dot-dashed line is the Pringle and Savonije (1979) temperature for a boundary layer dominated by electron scattering opacity.

In some cases of interest, electron scattering opacity dominates other opacity sources, and the boundary layer temperature is perhaps better approximated by (Pringle 1977):

$$T_{\text{BL}} \approx 7.6 \times 10^4 \left(\frac{\dot{M}}{10^{-5} M_{\odot} \text{ yr}^{-1}} \right)^{6/19} \times \left(\frac{M_1}{M_{\odot}} \right)^{8/19} \left(\frac{R_1}{R_{\odot}} \right)^{-18/19} \text{ K}. \quad (5)$$

These three relations for the boundary layer temperature have been plotted in Figure 1 as a function of accretion rate for a $1 M_{\odot}$ white dwarf and for a main sequence star. Except at low accretion rates onto a white dwarf, there are large differences between these estimates. In this study, we have adopted Lynden-Bell and Pringle's estimate as a reasonable compromise for the accretion rates of interest here.

Given the temperature structure in the accretion disk and the boundary layer, we can determine the emitted flux distribution. Recently, other investigators (e.g., Herter *et al.* 1979; Mayo, Wickramasinghe, and Whelan 1980) have used model atmosphere techniques to model the emergent flux from the accretion disk in cataclysmic variables. For the accretion rates considered here, the disk is optically thick and radiates locally very much like a blackbody (Williams 1980; Tylenda 1982). The boundary layer is generally thought to be optically thick, and since $T_{\text{BL}} \gtrsim 50,000$ K for most accretion rates we consider, we assume it also radiates as a blackbody. If we neglect extinction, the flux observed at Earth from accretion is:

$$F_A(\lambda) = \frac{2hc^2}{\lambda^5} \left(\frac{R_1}{d} \right)^2 \cos i \int_1^{R_2/R_1} \frac{2\pi x dx}{\exp [hc/\lambda kT(x)] - 1} + \frac{\pi + \gamma_0}{50} \left[\exp \left(\frac{hc}{\lambda k T_{\text{BL}}} \right) - 1 \right]^{-1}, \quad (6)$$

where

$$x \equiv R/R_1 \quad (7)$$

and

$$T(x) = \left(\frac{3GM_1\dot{M}}{8\pi\sigma R_1^3} \right)^{1/4} x^{-3/4} (1 - x^{-1/2})^{1/4}. \quad (8)$$

In this expression for the flux, we have introduced the possibility of viewing the disk at an angle other than pole-on ($i = 0^\circ$) by including a $\cos i$ term. We have followed Tylenda's (1977) formalism for the obscuration of the boundary layer by the central star with the term involving γ_0 . It is given by $\sin i \sin \gamma_0 \approx 0.1$.

b) Spectrum of the Nebula

The continuous spectrum emitted by a gaseous nebula consisting of hydrogen and helium has been discussed in detail by Brown and Mathews (1970). In general, the flux can be written as:

$$F_{\text{neb}}(\lambda) = \sum_i n_i n_e V \gamma_i(\lambda, T_e) / 4\pi d^2, \quad (9)$$

where γ_i is the emission coefficient, n_e is the electron density, n_i is the density of some ionized species, V is the volume of the gas, and T_e is its electron temperature. We define the number of H I and He II ionizing photons to be

$$N_\gamma(\text{H}) \equiv \int_0^{912 \text{ \AA}} \frac{\lambda L_h(\lambda)}{hc} d\lambda \quad (10)$$

$$N_\gamma(\text{He}^+) \equiv \int_0^{228 \text{ \AA}} \frac{\lambda L_h(\lambda)}{hc} d\lambda, \quad (11)$$

where $L_h(\lambda)$ is the luminosity of the hot component (accretion disk or blackbody) per unit wavelength interval. If we assume the nebula is optically thick in the continuum to all photons below the Lyman limit, but optically thin to photons above the limit, we may rewrite equation (9) as (cf. Osterbrock 1974, chap. 2):

$$F_{\text{neb}} = \frac{N_\gamma(\text{H})}{4\pi d^2 \alpha_B} \gamma_{\text{H}}(\lambda, T_e) + \frac{N_\gamma(\text{He}^+)}{4\pi d^2 \alpha_{\text{He}^+}} \gamma_{\text{He}^+}(\lambda, T_e) \quad (12)$$

where α_B and α_{He^+} are recombination coefficients for ionized hydrogen and doubly ionized helium, respectively. For a given gas temperature and density, then, our computed nebular continuum is the *maximum* possible for a given source of ionizing photons. We will not consider emission from He I in this study since the He I continuum is a factor of 10 weaker than the H I continuum (Osterbrock 1974).

Two emission processes will dominate the nebular continuum of a symbiotic star: free-bound and free-free emission. For the electron densities observed in most systems ($n_e \gtrsim 10^6 \text{ cm}^{-3}$), hydrogen two-photon emission will contribute a negligible amount to the total flux providing case B recombination is applicable (see below) (Drake and Ulrich 1981; Brown and Mathews 1970; Spitzer and Greenstein 1951). The free-bound emission coefficient is:

$$\gamma_{\text{fb}}(\lambda, T_e) = 6.48 \times 10^{-22} T_e^{-3/2} \lambda^{-2} \exp \left(-\frac{hc}{\lambda k T_e} \right) \times Z^4 \sum_n \exp \left(\frac{I_n}{k T_e} \right) \frac{g_{\text{fb}}(n, \lambda, T_e)}{n^3}, \quad (13)$$

where I_n is the ionization potential of the n th level of H I or He II, Z is the nuclear charge, and g_{fb} is the free-bound Gaunt factor. We write the free-free emission coefficient as:

$$\gamma_{ff}(\lambda, T_e) = 5.16 \times 10^{-30} Z^2 \left(\frac{Z^2 I_H}{kT_e} \right)^{1/2} \lambda^{-2} \times \exp \left(- \frac{hc}{\lambda kT_e} \right) g_{ff}(\lambda, T_e), \quad (14)$$

where I_H is the ionization potential of hydrogen and g_{ff} is the free-free Gaunt factor. Free-bound Gaunt factors are tabulated by Karzas and Latter (1961), and we use the expansion for the free-free Gaunt factor given by Seaton (1960):

$$g_{ff}(\lambda, T_e) = 1 + 0.1728 \left(\frac{hc}{\lambda Z^2 I_H} \right)^{1/3} \left(1 + 2 \frac{\lambda kT_e}{hc} \right) - 0.0496 \left(\frac{hc}{\lambda Z^2 I_H} \right)^{2/3} \left[1 + \frac{2 \lambda kT_e}{3 hc} + \frac{4}{3} \left(\frac{\lambda kT_e}{hc} \right)^2 \right]. \quad (15)$$

Our procedure for calculating the emission coefficients reproduces the tables of Brown and Mathews to better than 5%.

Symbiotic stars also display a rich emission line spectrum. The photon fluxes from the hot component can be used to predict the fluxes of the strong recombination lines of hydrogen Balmer series and He II. We write the line flux observed at Earth as:

$$F_{\text{line}} = \left(\frac{4\pi j_{\text{line}}}{n_i n_e} \right) (n_i n_e V) \left(\frac{1}{4\pi d^2} \right), \quad (16)$$

where j_{line} is the emission rate and n_i is the ion density. On the assumption made above that the nebula is radiation-bounded (optically thick to ionizing photons), we can replace the emission measure, $n_i n_e V$, using equation (10) for hydrogen Balmer lines or equation (11) for He II lines.

As a rule, symbiotic stars appear to possess substantial stellar winds from one or both components, and this circumstellar material no doubt is the source of most of the nebular emission. It seems reasonable to suppose, therefore, that the nebula has a density profile, $\rho \sim r^{-2}$, appropriate to the equation of continuity (at constant outflow velocity). Under these conditions, given typical density ranges ($n_e = 10^6$ – 10^{11} cm^{-3}) and velocity widths (≥ 500 km s^{-1}) observed in symbiotic stars, we estimate the optical depths in Ly α and H α in a radiation-bounded nebula to be $\sim 10^2$ – 10^3 and ~ 0.1 – 1.0 , respectively (cf. Cox and Mathews 1969). That is, conditions roughly appropriate to case B recombination are anticipated. In fact, the hydrogen Balmer line fluxes actually observed in symbiotic stars are generally consistent with this expectation (Bloch and Tchong 1951; Pagel 1958). We have therefore assumed conditions appropriate to optically thin (in the Balmer series) case B recombination. In some cases, the lower members of the Balmer series may be optically thick (Boyarchuk 1969). Our simple model does not strictly apply to these latter cases, but it should provide a useful guide for more complex models.

Our models include fluxes for eight Balmer lines (H α –H10) plus He II $\lambda 1640$ and $\lambda 4686$. The emission rates for the Balmer

lines and He II $\lambda 4686$ have been taken from Osterbrock (1974) for $n_e = 10^6$ cm^{-3} and $T_e = 10,000$ K; the He II $\lambda 1640$ rate is from Brocklehurst (1971) for the same conditions. We assume a full width of 600 km s^{-1} and a triangular line profile for each line in order to plot them over the continuous spectrum. This is comparable to the observed widths in most symbiotic stars (Anderson, private communication).

c) Spectrum of the Cool Component

Absolute spectral energy distributions of the late-type stars in our synthesized spectra were constructed by combining the relative flux distributions of O'Connell (1973) and MacFarlane (1979), which cover the optical spectrum, with UV data from Wu *et al.* (1980) and IR data from Johnson (1966) and Lee (1970) for giants with similar spectral types. In order to normalize these distributions, we proceeded as follows: a standard distance of 10 pc is assumed, and V magnitudes of -0.3 , -0.5 , and -0.5 assigned to K3, M2, and M4 giants, respectively. MacFarlane's data, which are well distributed over the B bandpass, were integrated over a B filter (Johnson 1965) and then fixed on an absolute scale by adopting the $B-V$ colors for giants given by Lee (1970) or Johnson (1966). O'Connell's relative fluxes were then normalized to those of MacFarlane and placed on an absolute scale as well. Fortunately, O'Connell's and MacFarlane's data agree within a few percent over the region 3600–6000 Å, so this should be a reliable normalization. The ANS UV fluxes of Wu *et al.* (1980) are then easily converted to the same absolute scale, as they share a common flux point with O'Connell's data at 3300 Å. The UV fluxes have in fact been extrapolated from 1550 Å (the shortest wavelength point of Wu *et al.*) down to 1000 Å; but since the giant never contributes a sizable flux shortward of 2600 Å, the accuracy of this extrapolation is unimportant. The flux distributions are then extended to 35,000 Å using Lee's and Johnson's JKL magnitudes.

d) The Combined Spectrum

We have chosen 96 points between 1000 and 35,000 Å as follows:

1. 1000–3300 Å: 24 points at 100 Å intervals plus three points for He II $\lambda 1640$;
2. 3400–10800 Å: 37 points from O'Connell including the important continuum points and absorption bands, 27 points for the Balmer and He II $\lambda 4686$ emission lines, and two points to cover either side of the Balmer jump at 3646 Å;
3. 10800–35000 Å: three points at J , K , L .

A standard distance of 10 pc is assumed, and our calculated fluxes for the hot component and the nebula are added to the observed fluxes of the cool star. The calculated flux in the J , K , L bandpasses has been integrated over the appropriate bandpass (Johnson 1965) to obtain correct JKL fluxes for the hot component and nebula.

III. SYNTHETIC SPECTRA

We now present our synthetic spectra for symbiotic stars. Two types of models have been considered: (i) those which are dominated by a hot dwarf star, and (ii) those which are dominated by accretion.

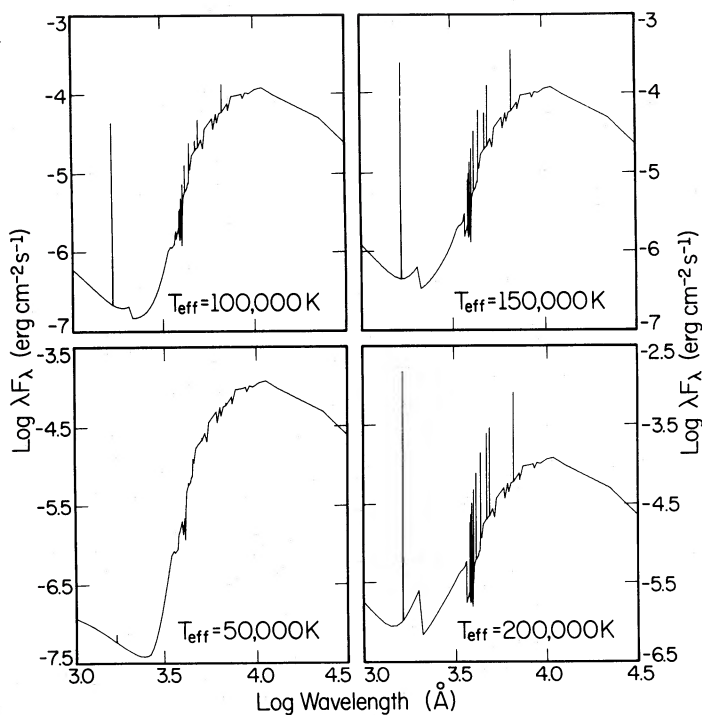


FIG. 2.—Synthetic spectra for a white dwarf ($R = 0.01 R_{\odot}$) at various effective temperatures in combination with an M2 III giant and a gaseous nebula. A distance of 10 pc is assumed for this and all subsequent synthetic spectra.

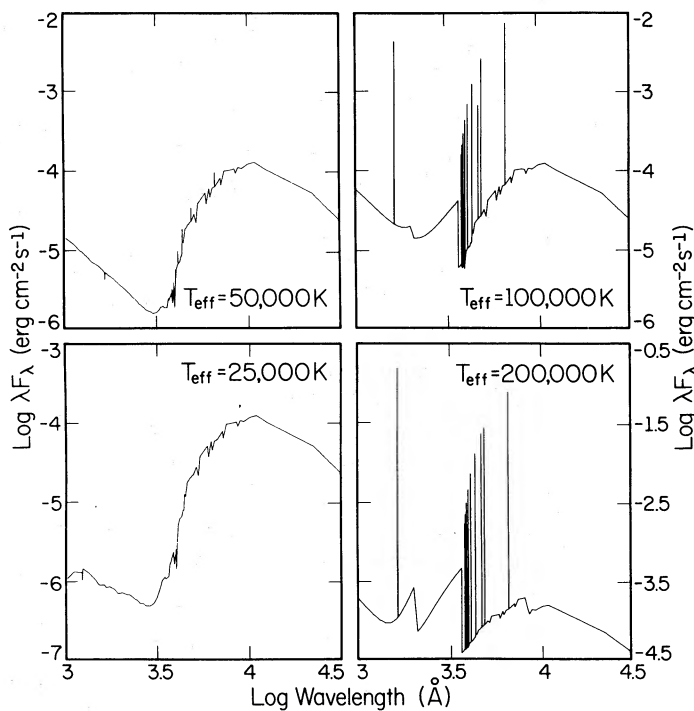


FIG. 3.—Synthetic spectra for a hot subdwarf ($R = 0.1 R_{\odot}$) at various effective temperatures in combination with an M2 III giant and a gaseous nebula

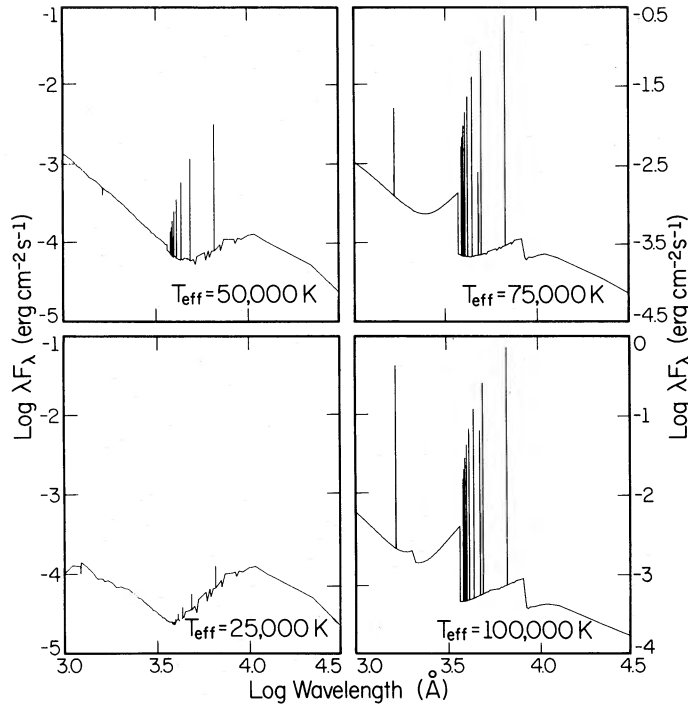


FIG. 4.—Synthetic spectra for a hot dwarf ($R = 1 R_{\odot}$) at various effective temperatures in combination with an M2 III giant and a gaseous nebula

a) Models with a Hot Dwarf Star

These spectra consist of a hot dwarf in combination with K or M giants and an ionized nebula. Examples of this type of model for a white dwarf secondary are shown in Figure 2. At low effective temperatures, the white dwarf spectrum is very weak compared to the M2 III companion. As we raise the white dwarf's temperature, the UV spectrum becomes increasingly dominated by nebular continuum radiation. At an effective temperature of 100,000 K, the He II $\lambda 1640$ line is very strong relative to the UV continuum, and there is a weak Balmer jump at $\lambda 3646$. The optical lines are fairly weak, and H β has an equivalent width of only 5 Å. The UV spectrum is quite remarkable at an effective temperature of 200,000 K: He II $\lambda 1640$ is extremely intense, and the jumps at $\lambda\lambda 2052, 3646$ are quite sharp. The optical spectrum, except for the bright emission lines, is not much different from a normal M giant. In this spectrum, H β has an equivalent width of ~ 50 Å, which is comparable to that observed in some symbiotic stars.

Two other sets of spectra are shown in Figures 3–4 for hot stars with larger radii. The behavior with increasing effective temperature is similar to that described above, although veiling of the giant's optical spectrum is much more pronounced. The Balmer jump is very noticeable in these spectra, and the He II $\lambda 2052$ edge appears for $T_h \approx 100,000$ K. At large radii ($R \approx R_{\odot}$), the entire spectrum is nebular radiation with only a trace of late-type absorption features. For comparison, Figure 5 is a spectrum of a $1 R_{\odot}$ blackbody and an M4 II giant (assumed to have $M_v = -2.5$). As we might expect, the hot component has a smaller effect on this brighter cool component. As before, the veiling of the absorption spectrum increases with increasing effective

temperature of the hot component. For extreme temperatures, the optical spectrum is primarily nebular, although some TiO bands are still visible.

As another comparison, the spectra in Figure 6 assume a nebular temperature of 20,000 K, rather than 10,000 K as assumed in earlier models. This modification has little effect on the UV continuum for $T_h \lesssim 50,000$ K, although the intensities of the emission lines are reduced slightly. The UV continuum is obviously much flatter as T_h increases beyond 75,000 K (compare with Fig. 3), and the magnitude of the jumps at $\lambda 2052$ and $\lambda 3646$ is reduced as well. At the highest effective temperatures ($T_h = 200,000$ K), the blue optical continuum from the hot component is very pronounced compared to spectra at lower electron temperatures, although the Paschen jump is much weaker.

b) Models with Accretion

These spectra consist of an accretion disk in combination with K or M giant primaries and an ionized nebula. Figure 7 displays four spectra for a $1 M_{\odot}$ main sequence star accreting material at the indicated rates from an M2 III companion with an assumed orbital inclination of 30° . At low rates, the optical spectrum is indistinguishable from a normal M2 giant, and the UV continuum is very weak. For these low rates ($\dot{M} \approx 10^{-7} M_{\odot} \text{ yr}^{-1}$), the system would not be classified as a symbiotic star at all, but rather as a normal Me variable (cf. Merrill 1940). For somewhat larger rates ($\dot{M} \approx$ a few times $10^{-7} M_{\odot} \text{ yr}^{-1}$), the nebular and Me-type Balmer lines will have roughly comparable intensities. Merrill (1921) noted this behavior in the peculiar Mira variable R Aquarii: Me-type H γ and H δ were strong at maximum light, while nebular H α and H β were conspicuous at minimum light. The

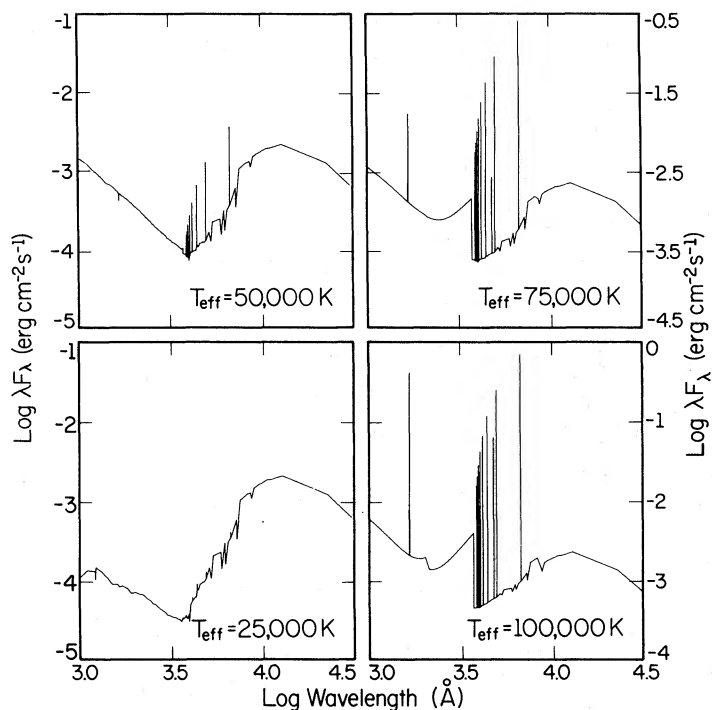


FIG. 5.—As in Fig. 4 but with an M4 II giant companion

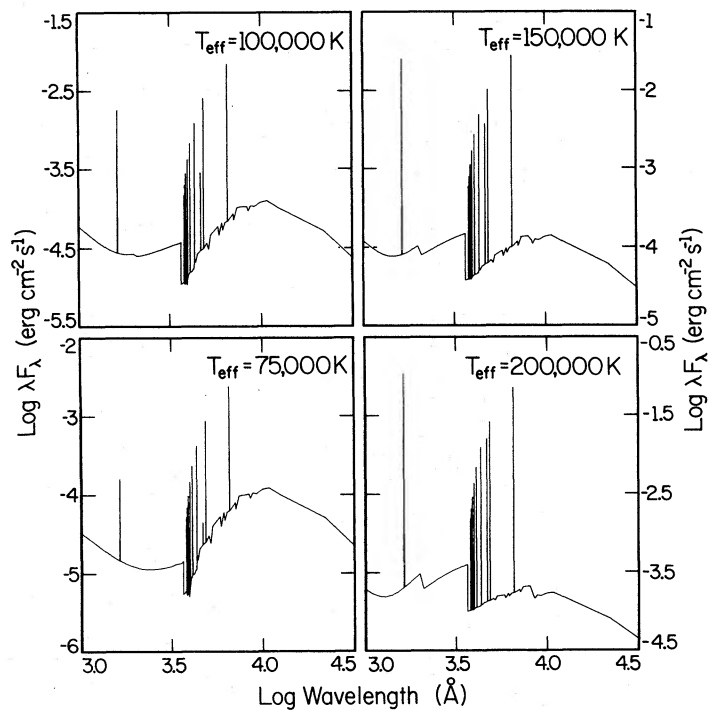


FIG. 6.—As in Fig. 3 but with an electron temperature, T_e , of 20,000 K

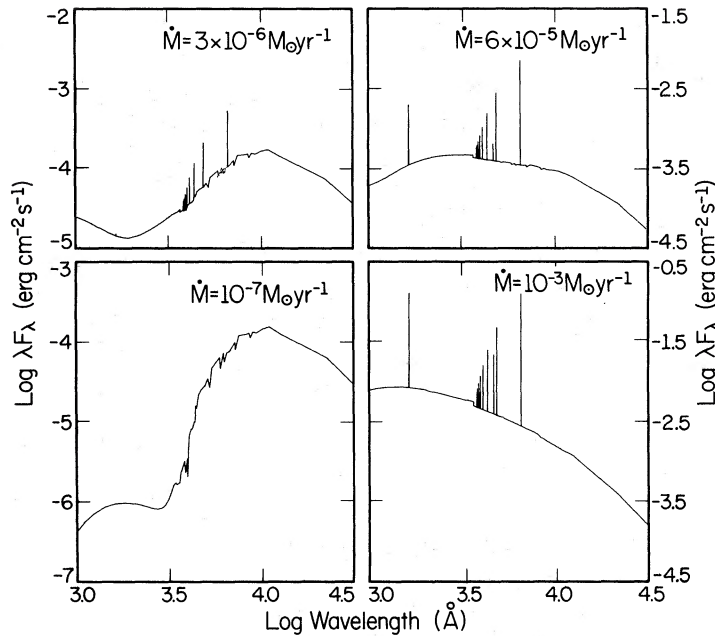


FIG. 7.—Four synthetic spectra of an accreting main sequence star ($M = 1 M_{\odot}$, $R = 1 R_{\odot}$) at an inclination of 30° in combination with an M2 III giant and a gaseous nebula.

accreting secondary does not announce itself in the optical until $\dot{M} \approx 10^{-6} M_{\odot} \text{ yr}^{-1}$; at these rates the Balmer lines are fairly strong and the spectrum appears composite. The blue veiling and the emission lines grow in strength as \dot{M} increases. At the highest allowed rates ($\dot{M} \approx 10^{-3} M_{\odot} \text{ yr}^{-1}$), the continuum is totally dominated by the disk and there is little evidence for a late-type giant.

The situation is quite different if the accreting star is a $1 M_{\odot}$

white dwarf (Fig. 8). Weak hydrogen Balmer and He II $\lambda 4686$ lines are visible even at very low accretion rates, and they strengthen markedly as \dot{M} increases. The Balmer jump is much more pronounced in the white dwarf accretor. This is a result of the deeper potential well which produces many more ionizing photons at a given accretion luminosity. At moderate accretion rates ($\dot{M} \approx 3 \times 10^{-8} M_{\odot} \text{ yr}^{-1}$) the UV spectrum resembles the blackbody models described earlier, especially

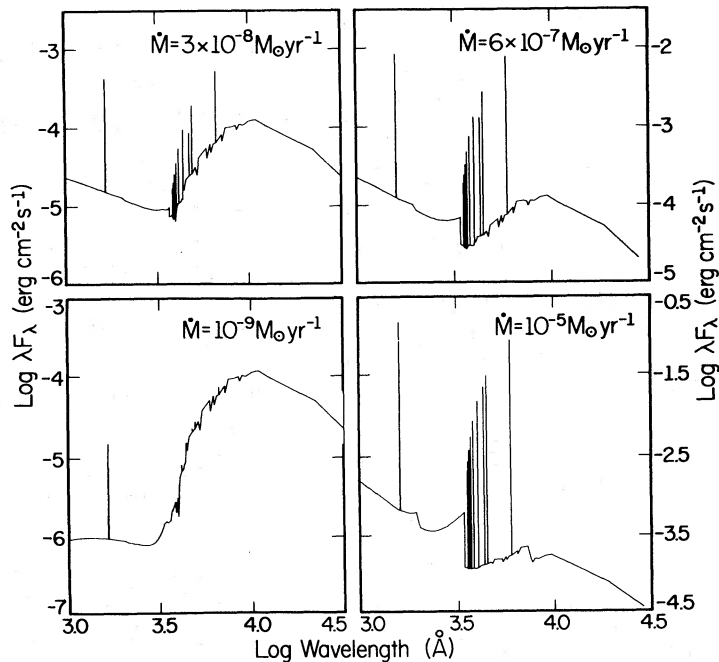


FIG. 8.—As in Fig. 7 for an accreting white dwarf ($M = 1 M_{\odot}$, $R = 0.009 R_{\odot}$, $i = 30^{\circ}$)

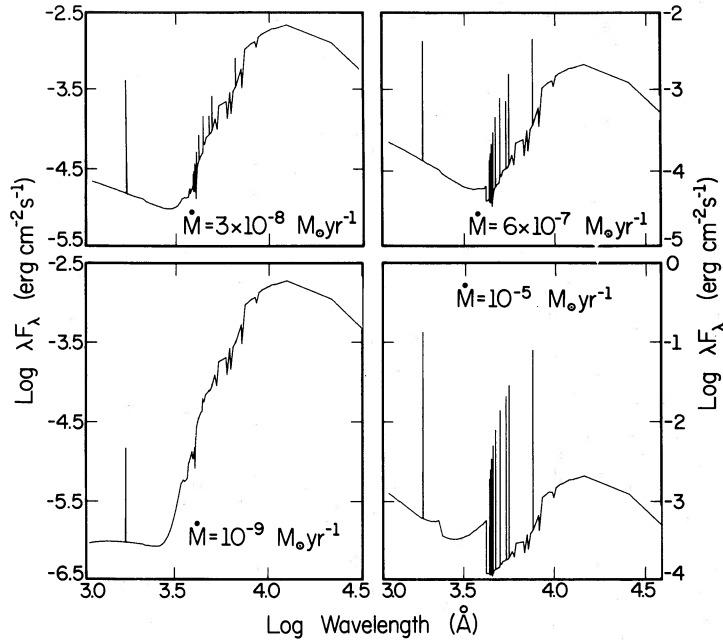


FIG. 9.—Synthetic spectra for an accreting white dwarf ($M = 1 M_{\odot}$, $R = 0.009 R_{\odot}$, $i = 30^{\circ}$) in combination with an M4 II giant and a gaseous nebula

if the system suffers some interstellar reddening. Even at the highest rates ($\dot{M} \approx 10^{-5} M_{\odot} \text{ yr}^{-1}$) the optical absorption features of the giant are still rather strong. The nebular emission is extremely intense at this accretion rate, and our approximation of optically thin emission lines is not valid (the computed equivalent width of $H\beta$ is nearly 1200 Å).

For comparison, Figures 9 and 10 plot synthetic spectra for M4 II companion stars. The presence of a bright giant does not affect the behavior of the white dwarf accretor (Fig. 9), although the late-type absorption spectrum is always

stronger for a given accretion rate. As before, the main sequence accretor is not recognized as an emission-line object until $\dot{M} \approx 10^{-6} M_{\odot} \text{ yr}^{-1}$ (Fig. 10). The equivalent width of $H\beta$ for this accretion rate is only 1.5 Å, and it would be difficult to distinguish this object from a normal M giant or Mira variable. Once the accretion rate reaches $10^{-5} M_{\odot} \text{ yr}^{-1}$, the optical spectrum is definitely composite and the UV continuum is disk-dominated. At very high accretion rates, the optical continuum has a color temperature near 10,000–15,000 K, and is similar to that seen in outburst for a symbiotic star.

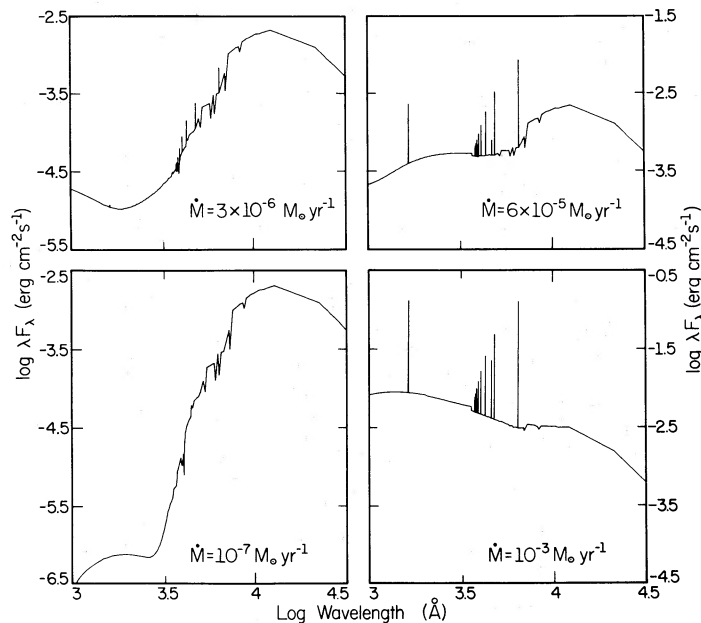


FIG. 10.—As in Fig. 9 for an accreting main sequence star ($M = 1 M_{\odot}$, $R = 1 R_{\odot}$, $i = 30^{\circ}$)

TABLE 1
OPTICAL CLASSIFICATION OF MODEL SYMBIOTIC STARS

Type of Hot Component	$N_{\gamma}(\text{H})^a$	Classification
Accreting white dwarf:		
$\dot{M} \lesssim 10^{-9} M_{\odot} \text{ yr}^{-1}$	$\lesssim 10^{44} \text{ s}^{-1}$	normal giant
$\dot{M} \gtrsim 10^{-9} M_{\odot} \text{ yr}^{-1}$	$\gtrsim 10^{44}$	symbiotic star
$\dot{M} \sim 10^{-5} M_{\odot} \text{ yr}^{-1}$	$\sim 10^{49}$	symbiotic star
Accreting main sequence star:		
$\dot{M} \lesssim 10^{-6} M_{\odot} \text{ yr}^{-1}$	$\lesssim 5 \times 10^{44}$	normal giant
$\dot{M} \gtrsim 10^{-6} M_{\odot} \text{ yr}^{-1}$	$\gtrsim 5 \times 10^{44}$	symbiotic star
$\dot{M} \sim 10^{-3} M_{\odot} \text{ yr}^{-1}$	$\sim 10^{48}$	F supergiant
Hot dwarf:		
$R = 0.01 R_{\odot}, T_{\text{eff}} \lesssim 75,000 \text{ K}$	$\lesssim 5 \times 10^{44}$	normal giant
$R = 0.1 R_{\odot}, T_{\text{eff}} \lesssim 50,000 \text{ K}$		
$R = 1 R_{\odot}, T_{\text{eff}} \lesssim 25,000 \text{ K}$		
$R = 0.01 R_{\odot}, T_{\text{eff}} \gtrsim 75,000 \text{ K}$	$\gtrsim 5 \times 10^{44}$	symbiotic star
$R = 0.1 R_{\odot}, T_{\text{eff}} \gtrsim 50,000 \text{ K}$		
$R = 1 R_{\odot}, T_{\text{eff}} \gtrsim 25,000 \text{ K}$		
$R \gtrsim 50 R_{\odot}, T_{\text{eff}} \lesssim 10,000 \text{ K}$		A-F supergiant

^a The number of hydrogen ionizing photons emitted by the hot component. The limits listed here refer to luminosity class III giants; the photon fluxes needed to produce a symbiotic spectrum are ~ 5 times larger for luminosity class II giants.

The emission lines are very strong in this object, but the optical continuum is remarkably reminiscent of an A-F supergiant.

IV. OBSERVATIONAL DIAGNOSTICS: THE CONTINUUM

The symbiotic stars were originally discovered as M giants with abnormally strong emission lines of hydrogen and helium. This simple definition for a symbiotic star has been applied to the *optical spectra* of our model binaries, and the results of this classification are listed in Table 1. A number of hot components do not emit enough high-energy photons to ionize the surrounding nebula. These systems have been classified as normal giants, although the *IUE* satellite would detect them as binaries. It is interesting that a wide variety of hot components can generate a symbiotic optical spectrum. An important question for us to ask now is: Do observational diagnostics exist which will allow us to discriminate among possible hot components in symbiotic stars? We have already seen that the UV continuum of our model binaries is determined solely by the hot component. We might also expect that the relative strengths of some emission lines (e.g., He II $\lambda 4686$ and H β) will depend on the nature of the hot component. In this section we examine continuum diagnostics, which measure the flux longward of 912 Å. Emission-line diagnostics, which measure the flux shortward of 912 Å, are discussed in § VI.

In our models, continuum radiation is emitted by a late-type giant, a hot component and an ionized nebula. For $\lambda \lesssim 3000$ Å, the flux from the hot component generally dominates the contribution from the nebula and the giant. In contrast, the *JKL* magnitudes are governed by the properties of the cool component, providing the optical luminosity of the hot component does not greatly exceed that of the giant. The importance of IR colors for determining the spectral class of the late-type giants in symbiotic stars has been reviewed by Allen (1979, 1982). Fortunately, the UV colors of our model symbiotic stars similarly allow us to ascertain the nature of the hot components.

a) UV Color Indices

We have characterized our models by continuum magnitudes ($m_{\lambda} = -2.5 \log F_{\lambda} - 21.10$) at four points: 1300, 1700, 2200, and 2600 Å. These points were chosen to span the continuum from the shortest wavelengths (~ 1300 Å) at which satellite observations with good signal-to-noise ratios are currently available to the longest wavelengths (~ 2600 Å) which still avoid any significant contribution from the late-type star. The point at 2200 Å was obviously chosen to exploit the characteristic interstellar absorption feature at that wavelength, thus allowing us in principle to separate the effects of interstellar reddening from differences in the form of the true underlying continuum. The remaining point, at 1700 Å, then affords relatively uniform sampling of the continuum at a point where the UV continua are usually strong. These four magnitudes we then use to define three color indices: $m_{1300} - m_{1700}$, $m_{1700} - m_{2600}$, and $m_{2200} - m_{2600}$. As discussed below, the second of these colors is the most sensitive to anomalies in the interstellar extinction curve. It is also the only index which requires flux measurements in both cameras of the *IUE*, and is thus the most vulnerable to calibration errors as well. The first and third indices, on the other hand, should be relatively insensitive to these effects.

Our color indices as functions of accretion rate and effective temperature are shown in Figure 11. The behavior of the model accretors is not a strong function of either the mass of the accreting star or the inclination, so our results

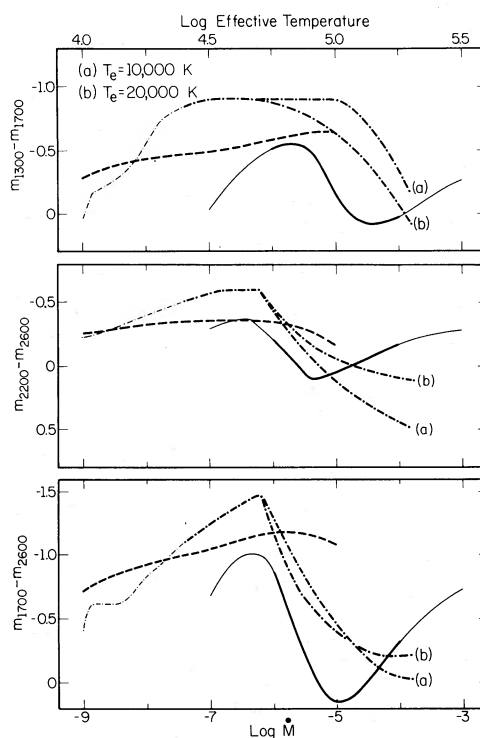


FIG. 11.—The behavior of $m_{1300} - m_{1700}$, $m_{1700} - m_{2600}$, and $m_{2200} - m_{2600}$ as a function of accretion rate and effective temperature for main sequence accretors (solid lines), white dwarf accretors (dashed lines), and hot stellar sources (dot-dashed lines). In this and subsequent figures, the range of models which are expected to have symbiotic optical spectra are drawn with dark lines.

are presented for $1 M_{\odot}$ accretors at $i = 30^{\circ}$. The results for hot star models assume a radius of $0.1 R_{\odot}$ for this component. Although the colors are insensitive to *increases* in the radius of the hot star, *early*-type giants may contribute a substantial 2600 Å flux for hot stars with smaller radii (e.g., white dwarfs).

The variations in the colors of main sequence accretors are due solely to changes in the accretion rate. As \dot{M} increases, the Planck peaks of the boundary layer and the disk migrate to shorter wavelengths (cf. eqs. [2] and [3]). Each of our UV colors first becomes progressively more negative, as the boundary layer peak passes shortward of its respective bandpass, then becomes more positive, as the peak of the disk itself encroaches on that bandpass, and finally becomes more negative again, as the peak of the disk passes shortward of the bandpass.

The UV colors of white dwarf accretors are much less affected by changes in \dot{M} since, for models which are recognizably symbiotic, the Planck peak of the disk already lies to the short wavelength side of our colors. In this limit, F_{λ} is asymptotically proportional to $\lambda^{-7/3}$ (Lynden-Bell and Pringle 1974). The nebular contribution to the flux at 2600 Å dominates the disk continuum for $\dot{M} > 10^{-7} M_{\odot} \text{ yr}^{-1}$, and this produces the turnover in $m_{2200} - m_{2600}$ and $m_{1700} - m_{2600}$ seen in Figure 11.

The nebular contribution is more pronounced in the hot star models, whose continua fall more steeply redward of the Planck peak. Balmer continuum radiation begins to dominate the stellar flux at 2600 Å when $T_h \approx 50,000$ K. At extreme temperatures ($T_h \gtrsim 100,000$ K), the Balmer and He II continua elevate the continuum at 1700 Å and 2600 Å with respect to 1300 Å and 2200 Å. Thus, the color indices of the hot stars become very red as T_h increases beyond 100,000 K.

b) Reddening-free Color Indices

The colors displayed in Figure 11 are unreddened, while the UV continua of most symbiotic stars have been affected by varying degrees of interstellar (and perhaps circumstellar) reddening. It is crucial, in any quantitative comparison of theoretical and observed continua of symbiotic stars, to fit simultaneously the reddening along with those parameters characterizing the intrinsic properties of the UV continua, because the relatively red intrinsic flux distributions of the accretion disk models can, under suitable circumstances, mimic those of more heavily reddened stellar sources. This phenomenon is illustrated by the panels at $\dot{M} = 3 \times 10^{-6} M_{\odot} \text{ yr}^{-1}$ in Figures 7 and 10. These are accretion rates quite typical of symbiotic star models which invoke accretion onto main sequence stars. In both spectra, F_{λ} displays a *minimum* near 2200 Å which is due *not* to interstellar reddening but to the existence of distinctly different peak temperatures characterizing the disk and boundary layer, whose flux maxima straddle the 2200 Å region. Similarly, the UV continua of most white dwarf accretors resemble moderately reddened blackbodies (cf. Figs. 8 and 9).

In order to minimize potential observational ambiguities between accretion models and more heavily reddened hot stellar atmospheres, we would like to construct reddening-free colors of the form:

$$C = (m_1 - m_2) - \beta(m_3 - m_4), \quad (17)$$

where $m_1, m_2, m_3,$ and m_4 are continuum magnitudes and β is given by

$$\beta = \frac{(A_3 - A_4)}{(A_2 - A_1)}. \quad (18)$$

The A 's are extinctions, in magnitudes, at the chosen wavelengths, according to a mean interstellar extinction curve.

Meyer and Savage (1981; see also Savage and Mathis 1979) have discussed the characteristics of the interstellar extinction curve over $\lambda\lambda 1550\text{--}3300$. They found significant variations in the shape of the UV extinction curve in some cases, and suggested that the average extinction curve may not be an infallible tool for dereddening UV spectra. However, their data do show that color excesses at 2200, 2500, and 3300 Å are well correlated. Additionally, color excesses at 1500 and 1800 Å appear to be well correlated with each other, but not with color excesses at longer wavelengths. Thus, while the shape of the UV extinction curve over $\lambda\lambda 1000\text{--}3300$ is variable, the relative slope in two regions ($\lambda\lambda 2200\text{--}3300$ and $\lambda \lesssim 1800$ Å) is preserved over large changes in E_{B-V} .

With these considerations in mind, we adopt the mean extinction curve of Savage and Mathis (1979) and define two reddening-free color indices:

$$C_1 = (m_{1300} - m_{1700}) - 0.46(m_{2200} - m_{2600}) \quad (19)$$

and

$$C_2 = 0.55(m_{1700} - m_{2600}) - 0.45(m_{1300} - m_{1700}). \quad (20)$$

In effect, the first of these, C_1 , measures the intrinsic *slope* of the far-UV continuum, and should be relatively insensitive to variations in the extinction curve or to calibration errors in the *IUE* flux measurements. Our second color index, C_2 , measures the *continuity* of the UV continuum across the 2200 Å extinction bump. This UV color is more vulnerable to variations in the extinction curve, since the extinction at 1700 Å may not be well correlated with that at 2600 Å.

The behavior of C_1 and C_2 for various types of hot components is shown in Figure 12. At low effective temperatures, the continua of the hot star models are dominated by the stellar component. Thus C_2 remains roughly constant for $T_h < 50,000$ K, while C_1 decreases monotonically with increasing temperature. Nebular radiation begins to contribute significantly to the 2600 Å flux once T_h reaches $\sim 50,000$ K. Recalling equations (19) and (20), C_1 will tend to decrease as m_{2600} gets brighter. On the other hand, C_2 tends to increase. As the effective temperature increases past 10^5 K, He II nebular radiation causes m_{1700} to brighten rapidly with respect to m_{1300} . The C_1 color index will tend to become more positive under these circumstances, while C_2 will decrease slightly.

The color indices displayed in Figure 12 do not show much of a variation for white dwarf accretors. The slow decrease in C_1 and C_2 at low \dot{M} represents a gradual steepening of the UV continuum with increasing \dot{M} . The large nebular contribution at 2600 Å causes C_1 (C_2) to rise (drop) slightly at high accretion rates.

C_1 and C_2 behave much differently for main sequence accretors. As we noted earlier, the boundary layer dominates the UV continuum of main sequence accretors for $\dot{M} \approx 10^{-7}$ to $10^{-6} M_{\odot} \text{ yr}^{-1}$. Once \dot{M} reaches $10^{-5} M_{\odot} \text{ yr}^{-1}$, the Planck peak of the boundary layer has moved into the far-UV,

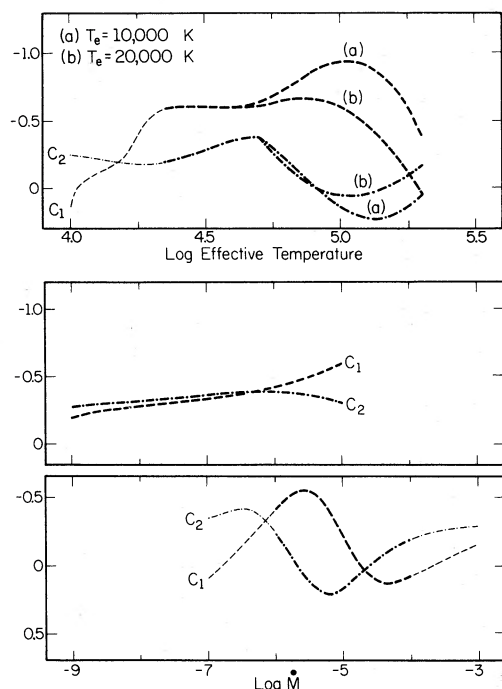


FIG. 12.—The behavior of the reddening-free color indices as a function of effective temperature and accretion rate for hot stars [top panel: (a) $T_e = 10,000$ K, (b) $T_e = 20,000$ K], white dwarf accretors [center panel], and main sequence accretors [bottom panel].

and, as the Planck peak of the disk passes shortward of 2000 \AA , both C_1 and C_2 become positive. At the highest accretion rates, the Rayleigh-Jeans tail of the disk dominates the UV, and the color indices decrease.

In Figure 12, we have seen that the C_1 and C_2 color indices are unique functions of either the accretion rate or effective temperature for each type of model symbiotic star. This is shown more effectively in Figure 13, which plots C_2 versus C_1 for each set of models. Once we define which of our models would be classified as symbiotic stars (cf. Table 1), we find that each class of model occupies its own region in the color-color plot. In particular, we have: (1) main sequence accretors: $C_1 \geq -0.5$, $-0.25 \leq C_2 \leq 0.25$; (2) white dwarf accretors: $C_2 \leq -0.25$, $-0.6 \leq C_1 \leq -0.2$; (3) hot stars: $C_1 \leq -0.5$, $C_2 \geq -0.4$. While these regions overlap somewhat, it appears that we can differentiate the hot components of symbiotic stars solely on the basis of their C_1 and C_2 colors.

The reader should bear in mind that the hot star track in Figure 13 is increasingly affected by Balmer continuum radiation for $T_h \geq 50,000$ K. If the circumstellar nebulae of symbiotic stars are density-bounded, or if they have significant optical depths in their continuum emission, rather than being radiation-bounded and optically thin as we have assumed, then we have overestimated the emitted nebular continuum flux. In this case, the leg of the hot star track from $(C_1, C_2) = (-0.6, -0.4)$ to the knee at $(C_1, C_2) = (-0.9, +0.1)$, which is due to the distortion of the 2600 \AA flux by Balmer emission, may be shortened, with the knee occurring at more negative values of C_2 . The location of the hot star track is also critically dependent on the nebular temperature, T_e , as T_h increases beyond $50,000$ K. As T_e

increases, the loop in the hot star track migrates to more positive C_1 values, as shown in Figure 13. Thus some knowledge of T_e may be necessary to determine accurately the nature of the hot components in some symbiotic stars.

c) Comparisons with Other Objects

As a test of our UV diagnostics, it would be highly desirable to compare our predicted colors with those of other objects of well-established nature which strongly resemble the hot components used in the synthetic spectra. For the hot stellar objects, the obvious counterparts are the planetary nebulae nuclei (although some important differences between our models and these objects exist, as discussed below). Similarly, classical novae at minimum provide a useful comparison for accreting white dwarf models (again with some important differences). Unfortunately, the postulated accretion rates needed to produce the symbiotic phenomenon with main sequence accretors have no known counterparts among other types of binaries: they are unique to the symbiotics.

i) Planetary Nebulae

In Table 2 we list the UV colors of six planetary nebulae for which integrated spectra (central star plus nebula) have been published: NGC 3242, NGC 6826, and IC 2149 (Perinotto and Benvenuti 1981a); NGC 7009 (Perinotto and Benvenuti 1981b); NGC 7662 (Benvenuti and Perinotto 1981); and IC 4997 (Feibelman 1982). The quoted uncertainties in the colors are the standard deviations between independent estimates of the continuum by the authors. Also listed in the tables are the logarithmic extinctions, $c_\beta = 1.47E_{B-V}$ (Seaton 1979), quoted in the published accounts of these spectra, and the hydrogen and helium Zanstra temperatures (Kaler 1983) determined from optical emission lines of the nebulae. The large difference in hydrogen and helium Zanstra temperatures for three of these nebulae (NGC 3242, NGC

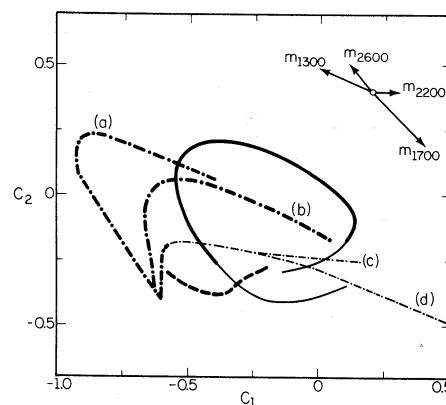


FIG. 13.—Color-color relation between C_1 and C_2 for main sequence accretors (solid line), white dwarf accretors (dashed line), and hot stellar sources (dot-dashed line). The branches of the trajectory for hot stellar sources refer, at high source temperatures, to nebular electron temperatures of (a) $T_e = 10,000$ K and (b) $T_e = 20,000$ K; at low temperatures, the branches define sequences at (c) constant luminosity ($\log L = 4$), appropriate to symbiotic stars in outburst, and (d) constant surface gravity ($\log g = 4$), appropriate to main sequence stars. The arrows in the upper right-hand corner of the diagram indicate the displacements in the position, of an object produced by increases in its brightness by $\Delta m = -0.2$ in each of the UV continuum points.

TABLE 2
ULTRAVIOLET CONTINUUM COLORS OF PLANETARY NEBULAE

Parameter	NGC 3242		NGC 6826		NGC 7009		NGC 7662		IC 2149		IC 4997	
	Thin	Thick										
$t_{\text{Ly}\alpha}$	0.22	0.04	0.27	0.04	0.27	0.04	0.23	0.33	0.23	0.33	0.39	0.39
c_{β}	4.71	4.53	4.64	4.53	4.64	4.53	4.79	4.48	4.79	4.48	4.81	4.81
$\log T_e(\text{H})$	4.94	...	4.89	...	4.89	...	5.03	...	5.03
$\log T_e(\text{He})$	7.85	6.78	8.44	6.78	8.44	6.78	9.34	8.40	9.34	8.40	11.31	11.31
$m_{1,700}$	± 0.01	± 0.02	± 0.01	± 0.02	± 0.01	± 0.02	± 0.05	± 0.04	± 0.05	± 0.04	± 0.07	± 0.07

UV Colors	NGC 3242		NGC 6826		NGC 7009		NGC 7662		IC 2149		IC 4997	
	Obs.	Model	Obs.	Model	Obs.	Model	Obs.	Model	Obs.	Model	Obs.	Model
$m_{1,300} - m_{1,700}$	-0.80	-0.70	-0.67	-0.83	-0.78	-0.65	-0.46	-0.69	-0.33	-0.57	+0.06	-0.54
	± 0.02	-1.23	± 0.01	-1.25	± 0.02	-1.21	± 0.01	-0.96	± 0.00	-0.97	± 0.01	-0.79
$m_{1,700} - m_{2,600}$	-1.15	-0.56	-1.19	...	-1.12	-0.68	-0.93	-0.33	-0.92	...	-0.04	-0.79
	± 0.07	-0.16	± 0.00	...	± 0.02	-0.07	± 0.03	+0.08	± 0.05	...	± 0.05	...
$m_{2,200} - m_{2,600}$	-0.46	+0.37	-0.47	-0.51	-0.19	+0.38	0.00	+0.55	+0.10	+0.08	+0.55	+0.45
	± 0.11	-0.63	± 0.03	-0.60	± 0.01	-0.82	± 0.00	-0.90	± 0.03	...	± 0.06	...
C_1	-0.58	-0.86	-0.45	-0.60	-0.69	-0.61	-0.46	-0.71	-0.38	-0.60	-0.19	-0.74
	± 0.05	-0.36	± 0.02	-0.31	± 0.02	-0.36	± 0.01	-0.23	± 0.01	...	± 0.03	...
C_2	-0.27	+0.02	-0.35	-0.31	-0.27	-0.06	-0.30	+0.12	-0.35	-0.27	-0.05	-0.20
	± 0.04	...	± 0.01	...	± 0.02	...	± 0.02	± 0.02	± 0.02	...	± 0.05	...

7009, and NGC 7662) indicates they are optically thin in the hydrogen Lyman continuum. The remaining three nebulae do not show helium emission lines, and so only hydrogen Zanstra temperatures are available. If the central stars of these latter planetaries are of average luminosity, their ionized nebular masses must be smaller than average (Kaler 1983), considerably so in the case of IC 4997. It is therefore likely that IC 4997 and probably also NGC 6826 and IC 2149 are optically thick to Lyman continuum radiation.

For comparison, we also list in Table 2 the UV colors predicted by our models for hot stars (plus nebulae) with effective temperatures equal to the measured Zanstra temperatures of these planetaries, together with the observed and calculated reddening-free color indices C_1 and C_2 . In the C_1 - C_2 diagram, all of the planetary nuclei (with the exception of IC 4997) fall near positions on the hot star track predicted from their hydrogen Zanstra temperatures, with $\langle(C_1, C_2)_{\text{obs}} - (C_1, C_2)_{\text{theor}}\rangle = (+0.12 \pm 0.06, 0.00 \pm 0.04)$. Furthermore, the reddened model UV colors in this case are also in very good agreement with those observed (given the additional uncertainty in the assumed reddening so introduced). The small systematic displacement of the (C_1, C_2) colors may be qualitatively understood in terms of hydrogen two-photon emission, which has been neglected in our models. This may be an important contributor to the flux at the lower densities appropriate to planetary nebulae, and tends to make its largest fractional contribution, relative to the model continuum, at 1700 and 2200 Å (between the rising Rayleigh-Jeans tail of the central star near 1300 Å and the rising nebular Balmer continuum near 2600 Å) producing a shift in the proper direction in the C_1 - C_2 diagram.

The hydrogen Zanstra temperatures, like our models of hot stars in symbiotic systems, assume the nebula is optically thick to Lyman continuum radiation, and it is therefore encouraging that our models are in substantial agreement with observations of planetary nebulae if we adopt the hydrogen Zanstra temperatures as the central star temperatures. If a nebula is optically thin in the hydrogen Lyman continuum, however, the helium Zanstra temperature is undoubtedly nearer the true stellar temperature. Our models then overestimate the Balmer continuum flux, and may considerably foreshorten the upward loop of the hot star tracks in the C_1 - C_2 diagram at high temperatures, as noted above. In this case, our models may lead us to underestimate the temperature of the hot star, but the important point is that they still clearly identify hot stellar components, separating them from accreting main sequence stars and, to a lesser degree, from accreting white dwarfs in the C_1 - C_2 diagram.

Planetary nebulae generally show strong infrared excesses, symptomatic of circumstellar dust emission, and this is true of the six objects we have sampled here (Gillett, Merrill, and Stein 1972; Cohen and Barlow 1974). One would therefore expect some degree of circumstellar extinction in each case. A useful measure of this extinction is $L_{\text{IR}}/L_{\text{Ly}\alpha}$ (Cohen and Barlow 1974); the ratio of infrared luminosity to the optically inferred nebular Ly α luminosity, which is a measure of the intrinsic hydrogen photoionization luminosity. For all the planetary nebulae sampled here except IC 4997, this ratio is small, $L_{\text{IR}}/L_{\text{Ly}\alpha} < 1$ (Cohen and Barlow 1974), and the UV colors show little evidence in the C_1 - C_2 diagram of anomalous reddening. IC 4997, on the other hand, has

$L_{\text{IR}}/L_{\text{Ly}\alpha} = 6.5$ (Cohen and Barlow 1974), and falls far from its predicted location in the C_1 - C_2 diagram. Its observed continuum shortward of 2200 Å is substantially weaker than that expected on the basis of its nebular Zanstra temperature and the strength of the 2200 Å absorption feature. We attribute this anomaly to additional extinction in the circumstellar envelope, which evidently has an unusually weak 2200 Å feature. IC 4997 is thus an obvious example of the dangers inherent in applying our diagnostics to objects showing evidence for a significant amount of circumstellar dust. We do not therefore regard the C_1 - C_2 diagram as a reliable diagnostic of the nature of hot components in symbiotic stars showing large infrared excesses, symptomatic of circumstellar dust.

ii) Old Novae at Minimum

The UV colors of three old novae at minimum, V603 Aql, HR Del, and RR Pic (Krautter *et al.* 1981), are listed in Table 3. As in Table 2, the quoted uncertainties in these colors are the standard deviations between independent estimates of the continuum by the authors. For each system listed in this table, an estimate of the mass accretion rate was derived by fitting the observed absolute flux at 1700 Å to that from an accreting white dwarf model, corrected for distance (McLaughlin 1960; Webbink and Gallagher, unpublished), extinction (Krautter *et al.* 1981), and orbital inclination (Ritter 1982). A ratio $R/M = 0.009 R_{\odot}/M_{\odot}$ was assumed for the accreting white dwarf. The model UV colors, appropriately reddened, are then listed for comparison in Table 3 along with the C_1, C_2 indices. The observed C_1, C_2 indices fall slightly above and to the left of those predicted by the model: $\langle(C_1, C_2)_{\text{obs}} - (C_1, C_2)_{\text{theor}}\rangle = (-0.17 \pm 0.06, +0.07 \pm 0.02)$, a difference which appears due to a slight excess flux at 1300 Å in the observed systems. Neither the

TABLE 3
ULTRAVIOLET CONTINUUM COLORS OF OLD NOVAE
A.

Parameter	V603 Aql	HR Del	RR Pic
d (pc).....	376	810	480
i (degrees).....	15	42	65
E_{B-V}	0.08	0.15	0.01
m_{1700}	9.76	9.75	9.65
	± 0.01	± 0.07	± 0.07
$\log \dot{M}$ ($M_{\odot} \text{ yr}^{-1}$).....	-8.69	-7.43	-8.00

B.

UV Colors	V603 Aql		HR Del		RR Pic	
	Obs.	Model	Obs.	Model	Obs.	Model
$m_{1300} - m_{1700}$	-0.60	-0.25	-0.44	-0.29	-0.60	-0.43
	± 0.06		± 0.01		± 0.04	
$m_{1700} - m_{2600}$	-0.91	-0.83	-0.88	-0.88	-0.86	-0.92
	± 0.07		± 0.01		± 0.04	
$m_{2200} - m_{2600}$	-0.16	-0.05	-0.10	+0.05	-0.41	-0.33
	± 0.11		± 0.06		± 0.07	
C_1	-0.52	-0.23	-0.39	-0.30	-0.42	-0.28
	± 0.08		± 0.03		± 0.05	
C_2	-0.23	-0.29	-0.29	-0.33	-0.20	-0.31
	± 0.05		± 0.01		± 0.03	

TABLE 4
ULTRAVIOLET COLORS OF SYMBIOTIC STARS

System (ℓ, b)	K Sp _g	Ref Ref	m_{1700}	m_{1300} - m_{1700}	m_{1700} - m_{2600}	m_{2200} - m_{2600}	C_1	C_2	SWP LWR	Ref	JD - 2440000 Date (UT)	m_v ϕ
Z And (110,-12)	5.00	KG83	11.76	-0.36					1485		3633.60	10.7
	M2	B67	± 0.03	± 0.02					-	A&81	5 May 78	0.30
	5.00	KG83			(a)	+0.88			-	A&81	3922.06	10.7
	M2	B67				± 0.01			3790		17 Feb 79	0.68
	5.00	KG83	11.63	-0.30	+0.22	+1.07	-0.79	+0.26	9940	V&82	4480.31	10.7
	M2	B67	± 0.13	± 0.16	± 0.12	± 0.16	± 0.17	± 0.10	8650		28 Aug 80	0.42
R Aqr (066,-70)	-0.5::	W&83a	12.37	-0.12	+0.26	+0.28	-0.24	+0.19	5938	MKH80	4080.59	10.6
	M7e	PG52	± 0.10	± 0.06	± 0.09	± 0.15	± 0.09	± 0.06	5166		25 Jul 79	0.42
TX CVn (131,+80)	6.30	KG83	10.50	+0.14	-0.53	-0.20	+0.24	-0.36	15655	S82	4943.74	9.8
	M0	MT78	± 0.01	± 0.02	± 0.07	± 0.06	± 0.03	± 0.04	12083		5 Dec 81	0.49
o Cet (168,-58)	-2.6:	C&79	12.82	+1.18					7796	WC79	4267.18	6.4
	M8.0e	J26	± 0.01	± 0.03					-		28 Jan 80	0.30
T CrB (043,+48)	4.77	KG83			(b)	+0.32			-	C&82	3953.72	10.1
	M3	K58				± 0.07			4082		21 Mar 79	0.34
	4.77	KG83	12.66	-0.28	-0.04	+0.22	-0.38	+0.10	5759	K&81	4064.68	10.0
	M3	K58	± 0.26	± 0.06	± 0.22	± 0.03	± 0.06	± 0.12	4995		10 Jul 79	0.81
	4.77	KG83	11.34	+0.06	-0.44	+0.24	-0.05	-0.27	9228	C&82	4399.47	10.0
M3	K58	± 0.06	± 0.06	± 0.03	± 0.05	± 0.07	± 0.03	7989	8 Jun 80		0.30	
	4.77	KG83	11.00	-0.30	-0.36	+0.20	-0.39	-0.06	13330	C&82	4652.98	10.0
	M3	K58	± 0.04	± 0.02	± 0.02	± 0.02	± 0.02	± 0.02	9929		17 Feb 81	0.41
BF Cyg (063,+07)	6.26	KG83	11.04	-0.24	-1.00	+0.51	-0.47	-0.45	8758	S82	4344.24	11.8
	M4	PG54	± 0.06	± 0.02	± 0.15	± 0.20	± 0.09	± 0.08	7501		14 Apr 80	0.66
CH Cyg (082,+16)	-0.7:	A82	9.52	+0.12					2163	HS82	3721.48	6.7
	M6	W42	± 0.03	± 0.17					-		31 Jul 78	0.64
	-0.7:	A82	8.99	+0.05	(c)				3983	HS82	3943.96	6.3
	M6	W42	± 0.00	± 0.01					4590		11 Mar 79	0.68
	-0.7:	A82	9.20	+0.47					5674	S82	4054.14	6.5
	M6	W42	± 0.13	± 0.01					-		29 Jun 79	0.70
	-0.7:	A82	9.52	+0.24					6606	HS82	4139.28	6.7
M6	W42	± 0.03	± 0.01					-	22 Sep 79		0.72	
	-0.7:	A82			(d)	+0.58			-	HS82	4221.70	6.8
	M6	W42				± 0.18			6392		13 Dec 79	0.73
	-0.7:	A82	7.66	+0.58					9983	S82	4484.19	6.4
	M6	W42	± 0.18	± 0.21					-		1 Sep 80	0.78
CI Cyg (071,+05)	4.46	KG83	12.10	+0.67	+0.48	+1.50	-0.02	-0.04	3816	St82	3879.36	10.2
	M4	A54	± 0.00	± 0.01	± 0.07	± 0.12	± 0.06	± 0.04	3396		5 Jan 79	0.39
V1016 Cyg (075,+06)	4.86	TY80	11.04	+0.04	+0.24	+0.58	-0.22	+0.11	5611	NS81	4049.46	10.8
	M6.5	MC75	± 0.11	± 0.10	± 0.05	± 0.04	± 0.10	± 0.05	4868		24 Jun 79	0.89
AG Dra (100,+41)	6.17	KG83	11.49	-0.68	-0.06	-0.03	-0.67	+0.28	5675	S82	4054.25	9.8
	K3	B66	± 0.13	± 0.12	± 0.16	± 0.20	± 0.15	± 0.10	4919		29 Jun 79	0.86
	6.17	KG83	8.92	-0.46	-0.24	+0.08	-0.50	+0.07	14640	A&82	4820.40	9.2
	K3	B66	± 0.01	± 0.01	± 0.02	± 0.04	± 0.02	± 0.01	11231		3 Aug 81	0.69
YY Her (048,+17)	7.97	KG83	13.34	-0.27	+0.22	+0.44	-0.47	+0.24	9773	M&82a	4464.16	13.0
	M2	H50	± 0.08	± 0.08	± 0.02	± 0.07	± 0.09	± 0.04	8493		12 Aug 80	-
V443 Her (051,+17)	5.37	KG83	11.20	-0.31	-0.28	+0.66	-0.62	-0.01	9122	St82	4385.46	11.5
	M3	TG58	± 0.02	± 0.07	± 0.01	± 0.12	± 0.09	± 0.03	7856		25 May 80	-

TABLE 4—Continued

System (l, b)	K Sp g	Ref Ref	m_{1700}	m_{1300} - m_{1700}	m_{1700} - m_{2600}	m_{2200} - m_{2600}	C_1	C_2	SWP LWR	Ref	JD - 2440000 Date (UT)	m_v ϕ
RW Hya (315,+36)	4.71 M2	KG83 M50	9.30 ± 0.05	-0.84 ± 0.01					5939 -	KMH80	4084.23 29 Jul 79	10.0: 0.59
	4.71 M2	KG83 M50			(e)	+0.07 ± 0.01			- 5481	KMH80	4117.84 1 Sep 79	10.0: 0.68
	4.71 M2	KG83 M50	9.56 ± 0.09	-0.94 ± 0.09	-0.56 ± 0.01	+0.10 ± 0.05	-0.98 ± 0.09	+0.11 ± 0.04	11000 9667	S82	4613.22 8 Jan 81	10.5: 0.01
BX Mon (220,+06)	5.82 M4	SA72 B54	14.04 ± 0.21	+2.02 ± 0.19	+1.48 ± 0.12	+1.52 ± 0.10	+1.33 ± 0.20	-0.09 ± 0.11	6344 5479	M&82a	4117.62 1 Sep 79	10.2 0.02
SY Mus (295,-04)	4.66 M2	FRC77 SS73	12.67 ± 0.01	+1.58 ± 0.08	-0.48 ± 0.11	+0.69 ± 0.40	+0.69 ± 0.20	+1.27 ± 0.07	10188 8855	M&82a	4503.52 21 Sep 80	11.2 0.94
	4.60 M2	FRC77 SS73	11.78 ± 0.13	-0.40 ± 0.11	+0.14 ± 0.04	+1.34 ± 0.08	-1.02 ± 0.11	+0.26 ± 0.05	14237 10828	M&82b	4766.96 11 Jun 81	10.8 0.36
AR Pav (329,-22)	6.91 M3	GW73 TH74	11.50 ± 0.11	+0.69 ± 0.30	-0.14 ± 0.30	+0.51 ± 0.13	+0.46 ± 0.30	-0.39 ± 0.21	13956 10570	S82	4735.39 10 May 81	10.2 0.37
AG Peg (069,-31)	3.92 M1.7	KG83 KP80	7.50 ± 0.01	-0.48 ± 0.04	-0.98 ± 0.04	-0.04 ± 0.01	-0.47 ± 0.04	-0.32 ± 0.03	2325 2101	KP80	3738.80 18 Aug 78	8.3 0.73
	3.92 M1.7	KG83 KP80	7.58 ± 0.03	-0.34 ± 0.03	-1.06 ± 0.04	-0.04 ± 0.12	-0.32 ± 0.06	-0.43 ± 0.02	5670 4915	S82	4053.87 29 Jun 79	8.3 0.11
	3.92 M1.7	KG83 KP80	7.74 ± 0.01	-0.70 ± 0.06	-0.72 ± 0.01	0.00 ± 0.05	-0.70 ± 0.06	-0.08 ± 0.03	6354 5490	S82	4118.60 2 Sep 79	8.4 0.19
RX Pup (258,-04)	2.73 M5	W&83b A80	12.05 ± 0.06	+1.62 ± 0.08	+0.68 ± 0.09	+2.16 ± 0.17	+0.62 ± 0.11	-0.35 ± 0.06	8762 7505	S82	4344.54 15 Apr 80	- 0.65
	2.18 M5	W&83b A80	12.14 ± 0.16	+1.38 ± 0.08	+0.62 ± 0.22	+1.89 ± 0.04	+0.52 ± 0.08	-0.29 ± 0.13	10189 8856	KMF82	4503.63 21 Sep 80	9.5: 0.92
CL Sco (352,+08)	7.85 K5	A82 A80	14.04 ± 0.12	+0.76 ± 0.05	+0.68 ± 0.15	+1.10 ± 0.69	+0.26 ± 0.32	+0.03 ± 0.08	9543 8296	M&82a	4440.04 19 Jul 80	12.8 0.89

NOTE. — Entries in successive columns are: (1) variable star name and galactic coordinates; (2) K magnitude of the system and spectral type of the cool component (For systems variable in the infrared, the magnitude quoted corresponds to the epoch or to the pulsation phase of the ultraviolet observation); (3) sources of the K magnitude and spectral type, respectively; (4) continuum magnitude at 1700 \AA (\pm standard deviation of two independent estimates, one by each author, of the continuum level); (5-7) ultraviolet continuum colors (\pm standard deviations as above); (8-9) reddening-free ultraviolet continuum colors (\pm standard deviations), as defined in the text; (10) exposure numbers (Short-Wavelength Primary and Long-Wavelength Redundant cameras) of the IUE spectra used to determine the continuum colors; (11) published source of the IUE spectra; (12) mean Julian date and UT date of the IUE spectra; and (13) visual magnitude and photometric/spectroscopic phase of the system at the epoch of observation. Visual magnitudes were provided, where available, by the American Association of Variable Star Observers (AAVSO) and the Variable Star Section of the Royal Astronomical Society of New Zealand (RASNZ); those for RW Hya and RX Pup are drawn from the combined IUE log. Ephemerides used to compute the phases in column (13) are discussed in the text.

(a) $m_{2600} = 11.50 \pm 0.01$

(b) $m_{2600} = 13.26 \pm 0.01$

(c) $m_{1700} - m_{2200} = +0.80 \pm 0.01$

(d) $m_{2600} = 7.71 \pm 0.14$

(e) $m_{2600} = 9.70 \pm 0.03$

REFERENCES:

A54	Aller 1954	B67	Boyarchuk 1967
A80	Allen 1980	C&79	Catchpole, et al. 1979
A82	Allen 1982	C&82	Cassatella, et al. 1982
A&81	Altamore, et al. 1981	FRC77	Feast, Robertson and Catchpole 1977
A&82	Altamore, et al. 1982	GW73	Glass and Webster 1973
B54	Bidelman 1954	H50	Herbig 1950
B66	Boyarchuk 1966a		

TABLE 4 (Continued)

HS82	Hack and Selvelli 1982	PG52	Payne-Gaposchkin 1952
J26	Joy 1926	PG54	Payne-Gaposchkin 1954
K58	Kraft 1958	S82	Slovak 1982
KG83	Kenyon and Gallagher 1983	St82	Stencel 1982
KMF82	Kafatos, Michalitsianos and Feibelman 1982	SA72	Swings and Allen 1972
KMH80	Kafatos, Michalitsianos and Hobbs 1980	SS73	Sanduleak and Stephenson 1973
KP80	Keyes and Plavec 1980	TG58	Tift and Greenstein 1958
K&81	Krautter, et al. 1981	TH74	Thackeray and Hutchings 1974
M50	Merrill 1950	TY80	Taranova and Yudin 1980
MC75	Mammano and Ciatti 1975	V&82	Viotti, et al. 1981
MKH80	Michalitsianos, Kafatos and Hobbs 1980	W42	Wilson 1942
MT78	Mammano and Taffara 1978	WC79	Wing and Carpenter 1979
M&82a	Michalitsianos, et al. 1982a	W&83a	Whitelock, et al. 1983a
M&82b	Michalitsianos, et al. 1982b	W&83b	Whitelock, et al. 1983b
NS81	Nussbaumer and Schild 1981		

models nor the observed systems are strongly affected by nebular continuum radiation. The excess flux observed at 1300 Å probably reflects a modest departure from the pure local blackbody disk assumed in our models. In reality, heavy blanketing by the Lyman continuum near temperatures of 10,000 K tends to redistribute flux from the blanketed region to wavelengths just above the ionization edge (e.g., Kurucz 1979). As with the planetary nebulae, however, the old novae fall near their anticipated locations in the C_1 - C_2 diagram, and are well separated from most accreting main sequence star models.

V. THE ULTRAVIOLET CONTINUA OF SYMBIOTIC STARS: APPLICATION TO OBSERVED SYSTEMS

a) Fitting of Model to Observed Ultraviolet Continua

Most of the bright symbiotic stars have now been observed with the *IUE* satellite. From the spectra available to us, we have selected those low-resolution spectra which are sufficiently well exposed to display a distinct continuum, and each of us has independently estimated the continuum magnitudes for each spectrum at the wavelengths defining our UV colors. The means and standard deviations of these estimates are listed in Table 4, together with data identifying the exposures measured, dates, and photometric or spectroscopic phases of the observations. In some cases,

multiple observations of a single object are available, and these are listed individually in Table 4. The reader should of course be aware that the choice of a continuum is a rather subjective process, particularly so for the many symbiotic stars which show very dense emission line systems in the ultraviolet; the uncertainties quoted in Table 4 reflect primarily the difficulty in defining the continuum, and not the true signal-to-noise ratios of the observations.

The reddening-free color indices calculated from the observed colors listed in Table 4 have been plotted on C_1 - C_2 diagrams in Figures 14-16. The vectors in the upper right-hand corner of Figure 13 illustrate the displacement in the position of an observed point resulting from an increase in brightness (decrease in magnitude) by 0.2 mag at each of the continuum points sampled. Because the errors in C_1 and C_2 may be highly correlated, we have represented each system by an error ellipse in Figures 14-16. The dimensions of the error ellipse represent one standard deviation; the 90% error ellipse is larger by a factor of 1.85. Four systems with multiple *IUE* observations (T CrB, AG Dra, AG Peg, and RX Pup) have been plotted separately in Figures 15 and 16.

Four systems listed in Table 4 are omitted from Figures 14-16: contemporaneous observations at all four continuum points are unavailable for *o* Cet B (= VZ Cet) and CH Cygni; BX Mon and SY Mus near photometric minimum both have large C_1 colors (symptomatic of a relatively cool UV continuum source) and fall outside the plot.

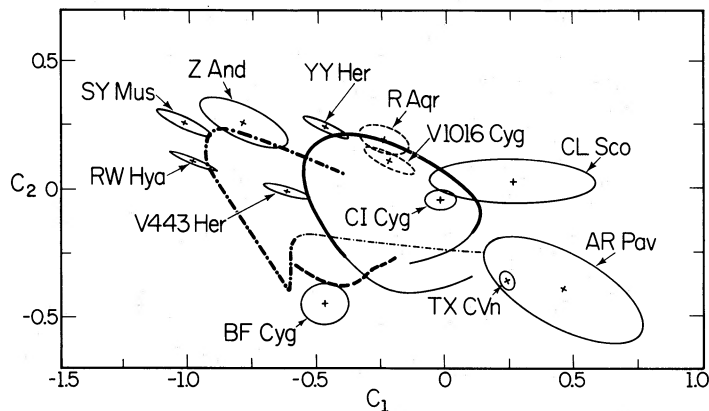


FIG. 14.—Color-color plot as in Fig. 13. The crosses indicate the positions of the symbiotic stars listed in Table 4, along with 1 σ error ellipses.

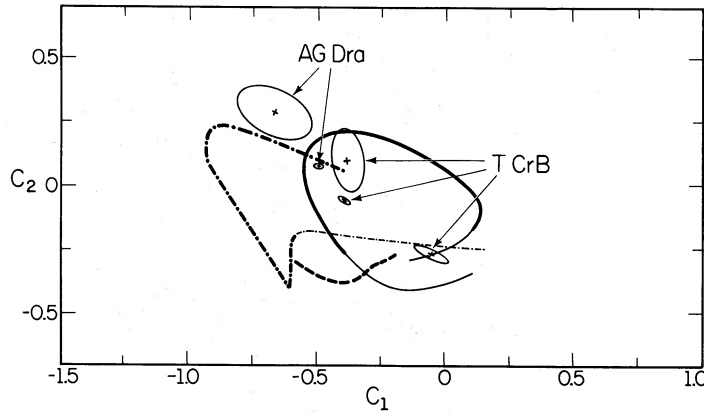


FIG. 15.—Color-color plot as in Fig. 13 showing multiple observations of T CrB and AG Dra

Three systems are plotted as dashed ellipses in Figures 14 and 16: R Aqr, V1016 Cyg, and RX Pup all show large excesses (Johnson 1982; Harvey 1974; Feast, Robertson, and Catchpole 1977, respectively), symptomatic of circumstellar dust emission. Stephens (1980) has shown that the amorphous silicates expected in red giant ejecta have different extinction properties from the particles which produce the average interstellar reddening. In these cases, as illustrated by the planetary nebula IC 4997 discussed above, our colors may no longer be truly reddening-free; solutions based on these colors may be fortuitous and misleading.

It is evident from Figure 14 that most of the symbiotic stars we have examined lie near only one of the sequences we have modeled. These systems then have unique solutions for the nature of the hot component, at least within the framework of our models. In a few cases, more than one solution may be possible: for these the derived reddening or predicted nebular spectrum will often serve to identify the correct model.

Table 5 lists, for each of the systems in Table 4, all best-fit solutions falling within the nominal 90% error ellipses in the C_1 - C_2 diagram. These solutions consist of a pair of parameters: a mass transfer rate, \dot{M} (for main sequence and white dwarf accretors), or an effective temperature, T_h (for hot stellar companions), obtained by fitting the (C_1, C_2) color

indices; and a color excess, E_{B-V} , derived by fitting the observed colors ($m_{1300} - m_{1700}$, $m_{1700} - m_{2600}$, and $m_{2200} - m_{2600}$) to the model colors. In a few cases, a value was assumed for E_{B-V} , as described below. We have assumed here that $M = 1 M_\odot$ for the accreting models, with $R = 1 R_\odot$ for main sequence stars and $R = 0.009 R_\odot$ for white dwarfs. Because the relative flux distributions of our model disks are functions only of $M\dot{M}/R^3$ (cf. eqs. [2], [3], and [12]), the derived accretion rates scale as R^3/M (providing the continuum of the giant companion makes a negligible contribution to the UV continuum).

The solutions listed in Table 5 rely, of course, upon a four-point characterization of the UV continuum. Many of them were therefore tested by fitting a large number (20–25) of UV continuum points to the model flux distributions discussed in § II. The nonlinear least squares algorithm employed in this parallel study is described by Kenyon (1983*b*), with results appearing elsewhere (Kenyon 1983*a, b*). The results of the more comprehensive fitting program are generally indistinguishable from those discussed here, with average differences in $\log \dot{M}$, $\log T_h$, and E_{B-V} of +0.02, +0.02, and -0.01, respectively. The C_1 - C_2 diagram thus appears to offer an accurate, reliable estimate of the solutions and parameters obtained from more detailed fits to the UV continua.

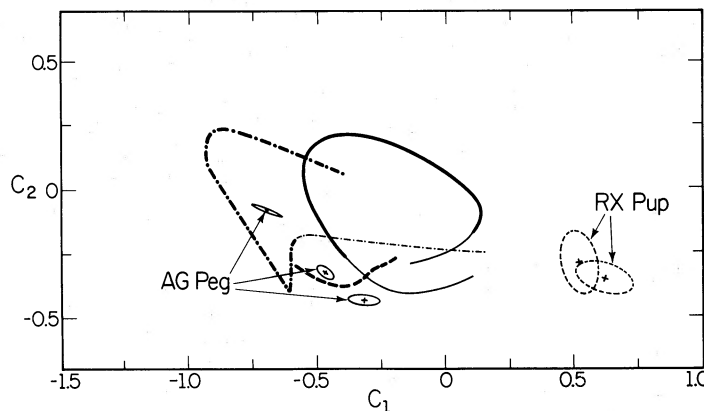


FIG. 16.—Color-color plot as in Fig. 13 showing multiple observations of AG Peg and RX Pup

TABLE 5
MODEL SOLUTIONS FOR INDIVIDUAL SYMBIOTIC STARS

System	Type ^a	Log \dot{M} ($M_{\odot} \text{ yr}^{-1}$)	Log T_h (K)	E_{B-V}
Z And	hs ₁	...	5.17 ± 0.04	0.27 ± 0.04
	ms	-5.43 ± 0.18	...	0.29 ± 0.10
	hs ₂	...	5.03 ± 0.12	0.38 ± 0.12
R Aqr	ms	-5.04 ± 0.09	...	0.08 ± 0.08
TX CVn	hs	...	3.985 ± 0.002	0.03 ± 0.03
o Cet B	hs	...	3.959	0.02^b
T CrB			no solution	
BF Cyg	wd	-6.00 ± 0.59	...	0.27 ± 0.03
	hs ₁	...	4.63 ± 0.10	0.49 ± 0.02
	ms	-6.28 ± 0.28	...	0.13 ± 0.09
CH Cyg			no solution	
CI Cyg	hs ₂	...	5.24 ± 0.03	0.57 ± 0.07
	ms	-4.40 ± 0.21	...	0.45 ± 0.02
V1016 Cyg	ms	-5.16 ± 0.17	...	0.17 ± 0.02
AG Dra (minimum)	ms	-5.36 ± 0.20	...	-0.09 ± 0.10
	hs ₁	...	5.19 ± 0.07	-0.08 ± 0.10
AG Dra (outburst)	hs ₂	...	5.04 ± 0.13	0.01 ± 0.15
	hs ₁	...	5.28 ± 0.01	-0.17 ± 0.03
YY Her	ms	-5.20 ± 0.08	...	0.13 ± 0.04
V443 Her	hs ₂	...	4.90 ± 0.02	0.31 ± 0.04
	ms	-5.72 ± 0.07	...	0.21 ± 0.09
RW Hya	hs ₁	...	4.95 ± 0.01	0.01 ± 0.02
BX Mon			no solution	
SY Mus	hs ₁	...	5.07 ± 0.03	0.38 ± 0.04
	hs	...	3.977 ± 0.007	0.28 ± 0.03
AR Pav	ms	-3.92 ± 0.75	...	0.26 ± 0.09
	hs	...	4.37 ± 0.04	0.17 ± 0.02
AG Peg	wd	-6.52 ± 0.17	...	0.13 ± 0.02
	hs ₂	...	4.76 ± 0.04	0.15 ± 0.04
RX Pup	hs	...	3.972 ± 0.003	0.87 ± 0.10
CL Sco	ms	-4.56 ± 0.11	...	0.52 ± 0.01
	hs ₂	...	5.19 ± 0.09	0.75 ± 0.17
	ms	-5.67 ± 0.24	...	0.99 ± 0.06

^a hs: hot star solution (hs₁: $T_e = 10,000$ K, hs₂: $T_e = 20,000$ K).

ms: main sequence accretor ($M = 1 M_{\odot}$, $R = 1 R_{\odot}$ assumed).

wd: white dwarf accretor ($M = 1 M_{\odot}$, $R = 0.009 R_{\odot}$ assumed).

^b E_{B-V} is assumed.

b) Discussion of Individual Systems

We turn now to a discussion of our solutions for individual systems:

1. *Z Andromedae*.—Our solutions for Z And are based on the ultraviolet colors from the *IUE* spectra of Viotti *et al.* (1982). These colors in fact differ little from the composite flux distribution obtained earlier by Altamore *et al.* (1981) by combining observations at two epochs nearly a year apart. According to Sahade, Brandi, and Fontenla (1981), however, the UV continuum shows substantial variability, and we have therefore applied our models quantitatively only to the observations by Viotti *et al.* (1982).

We obtain formal solutions both for hot stellar sources and for a main sequence accretor at the UV continuum source. Altamore *et al.* (1981) have fitted the UV continuum between 1200 and 2200 Å with a 43,000 K blackbody having a radius of 0.26 R_{\odot} . Our models indicate that such a low temperature cannot possibly produce enough Balmer continuum radiation to flatten the flux distribution longward of 2000 Å to the extent observed (cf. Fig. 3). A much better fit is given by a 100,000 K blackbody, as suggested

by Viotti *et al.* (1982). Such a strong photoionization source produces a substantial nebular continuum, but in this case a far stronger Balmer jump should be evident that that observed, given that the system is virtually as bright (even before correcting for extinction) at 2200 Å as it is at 5500 Å (compare Table 4, Fig. 3).

We are of the opinion that the main sequence accretor is most likely to be the correct solution. The optical emission line system of Z And is very similar to that of CI Cyg (discussed below as a prototypical main sequence accretor) when each is in quiescence, particularly in the great prominence of the [Ne v] and [Fe vii] emission line systems (see, e.g., Merrill 1950). This contrasts sharply with RW Hya and AG Dra (both of which we assign below to the class of hot stellar sources, and which straddle Z And in the C_1 - C_2 diagram), in which [Ne v] and [Fe vii] are weak or absent.

All of our solutions indicate that Z And is moderately heavily reddened ($E_{B-V} = 0.27$ to 0.38), in agreement with the estimates of Altamore *et al.* ($E_{B-V} = 0.30$) and Viotti *et al.* ($E_{B-V} = 0.35$) derived from the strength of the 2200 Å feature. According to the high-altitude extinction map of Burstein and

Heiles (1982), the asymptotic reddening in the direction of Z And is $E(B-V) = 0.24$. Circumstellar reddening is probably negligibly small. Taranova and Yudin (1981) reported a variable $10 \mu\text{m}$ excess in Z And, but infrared photometry by Woolf (1973) and by Eiroa, Hefele, and Qian (1982) reveals a stellar IR continuum with perhaps a small excess at $18\text{--}22 \mu\text{m}$ (Woolf 1973). This excess, even if real, is not strong enough to alter the observed reddening toward Z And materially.

Payne-Gaposchkin (1946) suggested a 694 day periodicity in the maxima and minima of Z And. By combining her photographic light curve with a visual light curve kindly supplied by the AAVSO covering the interval from 1923 to 1982, we find that the minima of Z And in quiescence are reproduced by the ephemeris:

$$\text{Min } (m_v) = \text{JD } 2,421,298 (\pm 15) + 756.85 (\pm 0.99) \cdot E,$$

which is the basis of the phases quoted in Table 4. Z And typically shows trains of outbursts of decreasing amplitude (see the light curve in Payne-Gaposchkin 1946). Within one such train, the interval between successive minima is somewhat shorter than when the system is at quiescence, in such a way that a train of outbursts generally has one additional minimum over its entire course beyond that predicted by the above ephemeris.

2. *R Aquarii*.—R Aqr is well known as a peculiar long-period variable embedded in a surrounding nebulosity (e.g., Kaler 1981; Michalitsianos and Kafatos 1982 and references therein). It is likely that internal reddening affects the UV continuum, as optical criteria give widely disparate estimates for E_{B-V} , from 0.0 to 0.5 (Johnson 1980, 1982; Wallerstein and Greenstein 1980). We consider it no more than coincidental, therefore, that R Aqr lies near the main sequence accretors in the $C_1\text{--}C_2$ diagram. Taken at face value, this solution would imply a distance of roughly 8 kpc to R Aqr (compared to Baade's [1943] expansion parallax of 260 pc) to account for the weakness of the UV continuum at such a high accretion rate, and $M_V = -4.2$ for the late-type component near pulsation minimum when it was observed.

The phases quoted in Table 4 are with respect to estimated visual maxima of the pulsating component on JD 2,443,910 and JD 2,444,319 (Mattei 1982). Willson, Garnavich, and Mattei (1981) have suggested that R Aqr is an eclipsing variable with an orbital period of 44 years: the epoch of observation corresponds to $\phi = 0.02$: on the putative eclipse ephemeris.

3. *TX Canum Venaticorum*.—This variable has been included in our study despite its extremely low excitation for a symbiotic star; Allen (1979) rejects it from his catalog on this account. It has been continuously at maximum visual light since late 1961 (Mammano and Taffara 1978), and the IUE observations by Slovak (1982) analyzed here thus reflect the outburst state.

Our derived temperature for the hot component is in excellent agreement with the B8–A0 spectral type assigned to it from optical spectra by Mammano and Chincarini (1966) and Fried (1980), as is the derived extinction with the value $E_{B-V} = 0.00$ from the H I maps of Burstein and Heiles (1982). The angular radius of the hot star, R_h/d , may be estimated by comparing the observed 1700 \AA flux with that of a Kurucz (1979) model atmosphere, and that of the cool

giant, R_g/d , by combining the observed K magnitude ($K = 6.30$; Kenyon and Gallagher 1983) with the effective temperature corresponding to its spectral type ($\sim M0$: Mammano and Taffara 1978) and the corresponding bolometric correction at K (Frogel, Persson, and Cohen 1981; Ridgway *et al.* 1980). This gives $\log R_h/R_g = -1.16 \pm 0.03$. The corresponding ratio of bolometric luminosities is $\log L_h/L_g = -0.74 \pm 0.07$.

The phases quoted in Table 4 for TX CVn follow the spectroscopic ephemeris of Fried (1980); defining phase $\phi = 0$ at periastron:

$$T_0 = \text{JD } 2,443,635 + 70.8 \cdot E.$$

We note, however, considerable scatter in the radial velocity curve, and both the orbital period and the extraordinary high orbital eccentricity ($e = 0.56$) deduced for this system require confirmation.

If the orbital period is correct and the giant is lobe-filling, then $R_g = 35 R_\odot$ (Kenyon and Gallagher 1983), which is typical of an M0 III giant (Allen 1973), and $R_h = 2.6 R_\odot$, which is normal for an A1 V star (Allen 1973). In light of the photometric and spectroscopic history of this variable, however, the hot star cannot be a main sequence dwarf. An attractive possibility is that it is the rejuvenated low-mass white dwarf remnant of the giant in a former Algol-type binary, reactivated in hydrogen shell burning at the onset of the second phase of mass transfer (cf. Nomoto, Nariai, and Sugimoto 1979; Webbink 1979). The white dwarf remnant masses should be strongly correlated with the final period of an Algol system (Refsdal and Weigert 1971). For $P = 71^d$ we estimate $M_{\text{wd}} = 0.30 M_\odot$, which is in good agreement with that implied by the core mass-luminosity relationship, $M_{\text{wd}} = 0.27 M_\odot$ (cf. Webbink 1975).

4. *o Ceti B = VZ Ceti*.—We include this, the visual companion to Mira (*o Ceti A*), as an extreme example of the symbiotic phenomenon. The visual orbit is not yet well established. Fernie and Brooker (1961) found that three possible orbits (periods 59, 169, and 261 years) fitted the then-available observations, but no subsequent solution has been attempted. VZ Cet shows variability on a 1000 s time scale (Walker 1957) and is believed to be accreting material from the stellar wind of Mira itself (Warner 1972; but note that it would seem to do so with extraordinarily high efficiency).

With only the short-wavelength spectra at hand, we have assumed a reddening of $E_{B-V} = 0.02$ to Mira, and corrected the observed m_{1300} and m_{1700} magnitudes by $+0.21$ and $+0.13$ mag, respectively, as an estimate (after Wu *et al.* 1980) of the contribution of *o Ceti A* to the ultraviolet flux. Our derived effective temperature, 9100 K, is in reasonable agreement with the spectral type B8 assigned by Joy (1926) to the optical continuum. The deduced angular radius, 4.3×10^{-6} arcsec, implies an absolute radius of $0.071 R_\odot$ for *o Ceti B*, assuming a trigonometric parallax of $0''.013$ (Jenkins 1952).

Phases quoted in Table 4 refer to visual maxima of *o Ceti A* on JD 2,444,164 and JD 2,444,504 (Mattei 1982).

5. *T Coronae Borealis*.—This erstwhile recurrent nova is included among some catalogs of symbiotic stars (e.g., Allen 1979, 1982). As such, it is one of the few systems with a

well-established spectroscopic orbit (Kraft 1958). Our phases in Table 4 refer to the epochs of spectroscopic conjunction (cool star in front):

$$\text{Conj} = \text{JD } 2,435,687 + 227.5 \cdot E$$

(Paczyński 1965), which also correspond to alternate minima in the system's ellipsoidal-like visual light curve (Bailey 1975).

That the giant in T CrB fills its Roche lobe is indicated by the classical symmetric, double-peaked profiles produced by an accretion disk, as seen in the Balmer emission lines (Kraft 1958). Of course, many other symbiotic stars also show double-peaked emission lines (e.g., Oliverson and Anderson 1982a), but in most cases the lines are very asymmetric, with the central minimum probably due to circumstellar absorption, rather than to an absence of emission (which is the case for an accretion disk). Confirmation of tidal mass transfer is found in the flickering displayed in the hot component of T CrB on ~ 100 s time scales (Walker 1957; Ianna 1964; Lawrence, Ostriker, and Hesser 1967). Webbink (1976) interpreted the outbursts of this system in terms of accretion events onto a main sequence star.

We can find no consistent solution for the observations at hand (Table 4) in terms of our models. The C_1 - C_2 colors of T CrB generally place it near the main sequence accretor track (cf. Fig. 15), but in fact the variations in these colors are not supported by the large, but uncorrelated, variations in the strength of the UV continuum, or by the singular lack of activity at visual wavelengths (see the last column of Table 4). Perhaps this large variability can be understood, at least qualitatively, in terms of transient hydrodynamic phenomena in a nonstationary accretion disk, which could be connected with the detection of T CrB as a weak X-ray source by the *Einstein* satellite (0.0083 ± 0.003 IPC counts s^{-1} [0.15–4.5 keV]; Córdoba, Mason, and Nelson 1981).

6. *BF Cygni*.—BF Cyg is among the lowest excitation systems of the "classical" symbiotics, with rather weak He II lines and no discernible higher excitation lines such as [Fe VII] and [Ne V] on optical spectra (Aller 1954; Boyarchuk 1969; Merlin 1972, 1973) or C IV $\lambda 1548$ on ultraviolet spectra (Slovak 1982). The optical light curve is quite regular; the ephemeris describing photographic minima,

$$\text{Min (pg)} = \text{JD } 2,415,065 + 757.3 \cdot E,$$

which was used to calculate the phases listed in Table 4 is that of Pucinskas (1970). The behavior of the light curve indicates that the system may undergo grazing eclipses, but these are not as regular as those seen in CI Cygni, for example.

We obtain three formal solutions for this system, but two of them can be rejected with some confidence. The accreting white dwarf model, while formally the best fit of the three, implies a much stronger nebular continuum and He II $\lambda 1640$ and $\lambda 4686$ emission (cf. Figs. 8 and 9) than observed. The accreting main sequence star model, on the other hand, implies very low foreground reddening to this system, $E_{B-V} = 0.13 \pm 0.09$. BF Cyg lies in field 267 in the galactic plane extinction map of Neckel and Klare (1980), which would place an object of this reddening at a distance of only 330 pc. The observed spectral type of the cool star is M4 III (Payne-Gaposchkin 1954), and the K magnitude

($K = 6.26$; Kenyon and Gallagher 1983), with appropriate correction for extinction, would imply a stellar radius of $\sim 12 R_{\odot}$ for the cool giant at this distance, far too small to fill its Roche lobe (at the apparent binary period) and feed a main sequence accretion disk.

The hot star solution is more satisfactory on several accounts, and is in accord with previous analyses by Boyarchuk (1969) and Slovak (1982). The implied reddening is consistent with the asymptotic reddening, $E_{B-V} = 0.45$, indicated beyond ~ 600 pc for this region of the sky in the extinction map of Neckel and Klare cited above. The observed ratio of 1700 Å to 2.2 μm flux for BF Cyg would then imply a ratio of stellar radii, $\log R_h/R_g = -1.89 \pm 0.04$ and of stellar bolometric luminosities $\log L_h/L_g = +0.53 \pm 0.16$. The equivalent widths of the nebular lines predicted by this solution also agree well with observations (see § VI, below).

7. *CH Cygni*.—CH Cyg is among the lowest excitation objects of all classical symbiotic stars, having been rejected on these grounds from Allen's original catalog (Allen 1979), although later restored (Allen 1982). Wallerstein (1968) and Cester (1968) first found the optical hot component to show rapid (~ 1 min) variability, a phenomenon since confirmed by many observers. In this respect, it differs from the canonical symbiotic stars such as Z And or AG Peg, for example: of the systems included in our study, only *o* Cet B and T CrB are known to display similar behavior.

CH Cygni also shows large-scale variations in its near-ultraviolet continuum (e.g., Hack and Selvelli 1982a), which probably arise from the same source as that responsible for its optical flickering. The lack of available simultaneous coverage of both long and short wavelength regions in the near-ultraviolet has prevented us from making any quantitative comparison to our models, but it seems safe to say that CH Cyg does not conform to any of them. The ultraviolet flux distribution is probably little affected by foreground reddening: Slovak and Africano (1978) estimate $E_{B-V} = 0.07 \pm 0.06$ from observations of nearby field stars, in agreement with $E_{B-V} = 0.03$ from the map of Burstein and Heiles (1982). This could conceivably be distorted by circumstellar reddening. CH Cyg is slightly variable at K (Allen 1982) and has a mild infrared excess at 10 μm and beyond (Gillett, Merrill, and Stein 1971; Morrison and Simon 1973), symptomatic of a circumstellar dust shell. We estimate that only 1%–2% of the total energy output of the giant appears in this infrared excess, but it still amounts to 5–10 times the power radiated by CH Cyg shortward of the Balmer jump. If the dust envelopes the entire system, however, and if it has absorption properties at all similar to interstellar grains, then the bulk of the energy radiated by the dust is reprocessed from the near-infrared continuum of the cool giant, rather than from the ultraviolet, and only a very small intrinsic reddening $(E_{B-V})_0 = 0.02$ is required. In this case, the increase in flux with increasing wavelength through the ultraviolet is probably real. Absorption features characteristic of late A or F stars are seen superposed on the ultraviolet continuum (e.g., Hack 1979; Hack and Selvelli 1982a, b; Hack, Persic, and Selvelli 1982) and the optical continuum (Kenyon 1983b; Wallerstein 1983). Although there is excess emission in the far-UV for such a star, as noted by Hack and Selvelli (1982b), the extremely low nebular excitation suggests that any underlying star is unlikely to be enormously hotter than this.

Although a main sequence companion to the giant is not excluded by the UV flux levels in CH Cyg, we are inclined to see a similarity between the behavior of its hot component and that of σ Cet B discussed above, albeit at a more intense level in this case. Further study is clearly required to elucidate the nature of this system.

In Table 4, the observations of this system are phased with respect to periastron according to the spectroscopic ephemeris proposed by Yamashita and Maehara (1979):

$$T_0 = \text{JD } 2,440,023 + 5750 \cdot E.$$

8. *CI Cygni*.—CI Cyg is one of two symbiotics generally acknowledged to undergo total eclipses (e.g., Hoffleit 1968), the other being AR Pavonis (although SY Mus, discussed below, should probably be added to this list). The phases quoted in Table 4 are computed with respect to mid-eclipse, according to Whitney's ephemeris (Aller 1954):

$$\text{Min} = \text{JD } 2,411,902 + 855.25 \cdot E.$$

The eclipse duration in CI Cyg requires the cool component to fill its tidal lobe, and CI Cyg has therefore been widely cited as an example of a symbiotic in which the outbursts are accretion-powered (e.g., Kenyon *et al.* 1982; Stencel *et al.* 1982; Bath and Pringle 1982; Iijima 1982).

While we obtain two formal solutions to the UV continuum of CI Cyg, the hot stellar solution can be dismissed with confidence. This solution gives a marginally better fit to the observed colors, but it also implies a much stronger nebular continuum and stronger He II $\lambda 1640$ and $\lambda 4686$ emission than is presently observed (cf. Fig. 4; Kenyon 1983*b*). Observations of the strong H I, He I, and He II optical recombination lines in CI Cyg indicate that this solution overestimates the luminosity of the hot component by a factor of ~ 10 (Kenyon 1983*b*).

Our remaining solution then clearly indicates that the source of the UV continuum in this system is an accretion disk surrounding a main sequence star. At the time of these observations, CI Cyg was in the late stages of decline from its 1975 outburst, and our estimate of the accretion rate, $\sim 2.5 \times 10^{-5} M_{\odot} \text{ yr}^{-1}$, is in reasonable accord with the theoretical models of Bath and Pringle (1982; see also Iijima 1982). That the outbursts are accretion-powered, reaching peak accretion rates well in excess of that determined here in late decline, is shown conclusively by an analysis of the 1975 eclipse (Webbink and Kenyon 1984). The interstellar reddening derived from our solution, $E_{B-V} = 0.45 \pm 0.02$, is in excellent agreement with the asymptotic reddening derived from neighboring field stars, $E_{B-V} = 0.45 \pm 0.05$, by Mikolajewska and Mikolajewski (1980), and with that derived from ratios of absolute line fluxes of lower members of the Balmer series (which are in emission), $E_{B-V} = 0.47 \pm 0.09$, by Iijima (1982).

9. *V1016 Cygni*.—V1016 Cyg and its sister object, HM Sge, are two of the most extreme examples of dusty symbiotic stars (cf. Webster and Allen 1975). Strong excesses are visible in the near-infrared (Swings and Allen 1972) and at 10–20 μm (Knacke 1972; Harvey 1974), indicating two components of hot circumstellar dust emission at temperatures of roughly 1000 K and 250 K (cf. Ahern *et al.* 1977 and references therein). V1016 Cyg is also detected as a radio source (Seaquist and Gregory 1973; Purton, Feldman, and

Marsh 1973) with a spectral index close to that appropriate for free-free emission in an outflowing wind ($F_{\nu} \propto \nu^{0.6}$; Wright and Barlow 1975); Ahern *et al.* (1977) derive an outflow rate of $1.5 \times 10^{-6} (d/1 \text{ kpc})^2 M_{\odot} \text{ yr}^{-1}$ from a combination of available radio data. High-resolution VLA data obtained at 1.3 cm by R. T. Newell (Newell and Hjellming 1981; Hjellming and Bignell 1982) reveal a distinctly bipolar appearance to the emission region, which has been interpreted by Kwok (1982) as the expanding wind from the hot component. Finally, Allen (1981) detected the system as an X-ray source with an observed flux in the 0.2–2 keV region of $7.5 \pm 3 \times 10^{-14} \text{ ergs cm}^{-2} \text{ s}^{-1}$.

Although V1016 Cyg has been widely discussed as a single-star progenitor of a planetary nebula (e.g., Nussbaumer and Schild 1981 and references therein), evidence for a cool component persists. Prior to its outburst in 1964, V1016 Cyg was noted as an emission object (MH α 328-116 = AS 373; Merrill and Burwell 1950) and also a long-period variable with late M-type absorption features (No. 39 in the list of newly discovered variables of Nassau and Cameron 1954). It has remained in outburst since 1964, and continues to show M-type absorption features in the red (TiO and VO bands; Mammano and Ciatti 1975; Andrillat, Ciatti, and Swings 1982) and in the infrared (CO and H₂O bands; Puetter *et al.* 1978). Harvey found the star to be periodically variable in the infrared; by phasing his observations with those of Yudin (1982) we derive the ephemeris at K:

$$\text{Max} (K) = \text{JD } 2,444,101 + 472 \cdot E,$$

to which the phases quoted in Table 4 refer.

We can attach no significance to our solution fitting the UV continuum of V1016 Cyg with that of an accretion disk surrounding a main sequence star; the observed optical continuum is far too weak to be consistent with this solution. We noted above that spurious results are possible if our UV diagnostics are applied to systems affected by circumstellar reddening, as is clearly the case here. Nevertheless, it appears the UV continuum of V1016 Cyg from 1200 to 3000 Å must be truly flat ($m_{\lambda} \sim \text{constant}$, to within 0.3 mag or so); Nussbaumer and Schild (1981) offer several independent reddening estimates based on their UV spectra. Those based on an adopted nebular model or a standard extinction curve are subject to error, but it is difficult to see how the differential reddening estimate derived from the [Ne v] $\lambda 1575/\lambda 2973$ intensity ratio could be seriously in error. This corresponds to $E_{B-V} = 0.20 \pm 0.10$ for a standard reddening curve, and is comparable with the asymptotic interstellar reddening ($E_{B-V} = 0.3$) beyond 1 kpc in this region (No. 285) of the extinction map by Neckel and Klare (1980). The UV source in V1016 Cyg thus has the appearance of being remarkably unattenuated by the dust radiating in the infrared. Given the weakness of the optical continuum in this object, we are inclined to concur with the conclusion of Nussbaumer and Schild (1981) that a hot stellar source is responsible for its strong emission line system: they estimate $\log T_h = 5.20$ and $E_{B-V} = 0.28$ from the ratio of H I to He II recombination line strengths. The ratio of observed X-ray flux (0.2–2 keV) to 1300 Å UV flux density is satisfied by a blackbody of the same temperature, $\log T_h = 5.20 \pm 0.03$, if we adopt their reddening estimate and allow for circumstellar X-ray attenuation. The intrinsic flatness of the UV continuum may then

be a result of reprocessing of the emergent flux in an optically thick stellar wind (cf. Cassinelli 1971; Harkness 1979), the existence of which is indicated by the radio spectrum.

10. *AG Draconis*.—The first observation of AG Dra summarized in Table 4 was obtained with the system at minimum in late June of 1979, more than 1 year prior to its recent outburst, while the second observation was made in 1981 August, during the decline from maximum. AG Dra is the only symbiotic star for which we have both pre-outburst and post-outburst ultraviolet spectra, and it therefore represents a unique opportunity to determine the cause of outburst. The phases quoted in Table 4 are based on the ephemeris derived by Meinunger (1979) describing its periodic variability in the near-ultraviolet:

$$\text{Max } (U) = \text{JD } 2,438,900 + 554 \cdot E .$$

This undoubtedly reflects modulation of the Balmer continuum emission which is very strong in this system; corresponding variations at *B* and *V* are much weaker (Meinunger 1979; Oliverson and Anderson 1982*b*). About 5 months prior to its optical outburst, AG Dra was also detected as an X-ray source, with $F_x = 2.8 \times 10^{-12}$ ergs cm^{-2} s^{-1} (0.2–2 keV; Anderson, Cassinelli, and Sanders 1981).

Although models involving rotational modulation of active surface regions on a single late-type giant have been discussed for AG Dra (Oliverson *et al.* 1980), its strong UV continuum clearly indicates the presence of a second, hot, component. Of the solutions which we list in Table 5 both during quiescence and in outburst, only that identifying the UV source as a hot star with a high electron temperature nebula surrounding it (hs_2) gives a consistent, nonnegative reddening to the system. Indeed, the deduced reddening is completely consistent with the high-latitude reddening map of Burstein and Heiles (1982), which indicates an asymptotic value through the galactic disk of $E_{B-V} = 0.03$ in this direction. A hot stellar UV source is also indicated by the very large Balmer jump in emission seen in this system, a jump which is markedly stronger than any observed in the systems we identify as main sequence accretors.

A somewhat higher temperature for the hot component is required to explain the observed X-ray flux as thermal emission from its surface: fitting the observed 0.2–2 keV X-ray flux and 1300 Å flux density at quiescence to a blackbody (assuming no foreground attenuation), we estimate $\log T_h = 5.22 \pm 0.02$. The difference between this estimate and the value listed in Table 5, $\log T_h = 5.04 \pm 0.13$ (hs_2), can probably be reduced by adopting an intermediate nebular electron temperature, which will tend to *increase* the derived hot star temperature, and *decrease* the derived reddening. For the colors given in Table 4 for the quiescent system, a small decrease in the assumed nebular temperature would reduce the derived reddening to $E_{B-V} = 0.0$, while increasing the derived T_h to a value more in accord with that needed to explain the X-ray observations, and at the same time satisfying emission measure constraints derived from the absence of certain coronal lines (Anderson *et al.* 1982).

The hot star solution listed in Table 4 for the system in quiescence (hs_2) implies a ratio of hot to cool star radii, $\log R_h/R_g = -3.14 \pm 0.37$, from fitting the relative fluxes at 0.13 and 2.2 μm and assuming a K3 III spectral type for the giant component (Boyarchuk 1969), with a corresponding ratio

of bolometric luminosities, $\log L_h/L_g = -0.64 \pm 0.37$. In this case, for a normal K3 III giant with $R = 20 R_\odot$ ($d = 0.6$ kpc), the hot star is clearly a hot white dwarf, $R_h \sim 0.014 R_\odot$. However, AG Dra is also a high-velocity star, $v_r = -140$ km s^{-1} (Roman 1953; Eggen 1964; Wallerstein 1981; Huang 1982) and shows many intense interstellar absorption lines (Altamore *et al.* 1982; Huang 1982). Roman (1953) considered the cool component a K1 II star, K0 Ib according to Huang (1982), and the brighter luminosity class is not only more typical of halo-population giants, but is in accord with the small proper motion observed for this star: $\mu = 0''.016$ yr^{-1} (AGK3 +66°715; AG Dra is also identical with SAO 016931, which gives $\mu = 0''.047$ yr^{-1}). In this case, the radii of the components and the distance to AG Dra are probably a factor of 4 or so greater, placing it ~ 2 kpc out of the galactic plane. Furthermore, the cool star then fills the better part of its Roche lobe, for which we estimate a radius of $\sim 120 R_\odot$, assuming a 554 day orbital period and total mass $\sim 1.5 M_\odot$.

Ultraviolet observations secured by Altamore *et al.* (1982) during the decline from its 1980 maximum show the UV continuum of AG Dra to be ~ 2.4 mag brighter, with little change in shape. They note that while the N v, C iv, and Si iv UV emission lines all increased in strength compared to pre-outburst spectra, they showed little evidence of a change in their relative intensities (although He II $\lambda 1640$ shows a smaller increase in intensity). In the optical region, the outburst is most marked in the nebular emission components, which have amplitudes comparable to that of the UV continuum, and the He II $\lambda 4686$ to H β ratio increases (Kaler 1980, 1983). Qualitatively, this behavior may be interpreted as reflecting a significant increase (factor of 2–3) in the photometric radius of the hot component during outburst, coupled with a modest increase in its temperature, implying that it lies near the high-temperature extreme of its track in the H-R diagram. This interpretation is supported by our outburst solution, $\log T_h = 5.07 \pm 0.01$, with $\log R_h/R_g = -2.66 \pm 0.03$, and $\log L_h/L_g = +0.45 \pm 0.05$.

The 1980 outburst of AG Dra appears to be substantially less developed than the large-scale thermonuclear events described below in § VII. However, as noted by Paczyński and Rudak (1980) and by Kenyon and Truran (1983), small-scale thermonuclear events can occur in a nondegenerate white dwarf envelope. In these outbursts, the hot white dwarf never develops an extended envelope, but remains at high effective temperatures throughout the runaway. The behavior of AG Dra suggests that the hot component lies near the high temperature extreme of its track in the H-R diagram, and has a mass of 0.7–0.8 M_\odot . Our estimated radius of the giant, $120 R_\odot$, implies a hot star luminosity, $L_h \approx 10,000 L_\odot$, which is in good agreement with that implied from a core mass-luminosity relation for a 0.7–0.8 M_\odot white dwarf, $L_h \approx 10,000$ – $16,000 L_\odot$.

11. *YY Herculis*.—This relatively neglected symbiotic star is optically rather similar to CI Cyg and AX Per (although somewhat fainter), with strong He II $\lambda 4686$ and prominent TiO bands in the optical (Herbig 1950), and strong N v, C iv, and [Mg v] present in the UV (Michalitsianos *et al.* 1982*a*). Michalitsianos *et al.* were unable to find a combination of hot star plus nebular continuum which gave a satisfactory fit to the UV continuum. Our diagnostics reaffirm this problem, but we obtain quite a satisfactory fit for a main sequence

accretor with $\dot{M} \approx 1.6 \times 10^{-5} M_{\odot} \text{ yr}^{-1}$. The deduced reddening for this model, $E_{B-V} = 0.13 \pm 0.04$, is in excellent agreement with the asymptotic reddening in the direction of YY Her using the extinction map of Burstein and Heiles (1982: $E_{B-V} = 0.15$). For a nominal orbital inclination of 30° , the strength of the UV continuum implies a distance of 5.5 kpc to YY Her, and an absolute magnitude of the late-type giant, $M_V = -0.77$, nearly normal for an M2 III giant (Herbig 1950). Our solution implies that this giant is lobe-filling, which would in turn imply that YY Her has a relatively short orbital period, $P \approx 150\text{--}200$ days.

12. *V443 Herculis*.—Little work has been done on this high-velocity symbiotic star since the spectroscopic study by Tift and Greenstein (1958). The main sequence accretor solution in Table 5 implies a derived reddening, $E_{B-V} = 0.20 \pm 0.09$, which is in good agreement with that indicated in the Burstein and Heiles (1982) reddening map, $E_{B-V} = 0.17$. However, the observed strength of the UV continuum would imply a distance of only ~ 0.9 kpc to V443 Her, and an absolute magnitude of only $M_V \approx +1$ for the system, rather faint to include a normal M giant. As noted by Tift and Greenstein (1958), the small proper motion of this object ($\mu = 0''.009 \pm 0''.007 \text{ yr}^{-1}$), coupled with its large negative radial velocity ($v_r = -60.4 \pm 2.3 \text{ km s}^{-1}$), suggests a much greater distance and a luminosity more appropriate to a metal-poor M giant.

We therefore consider the hot stellar solution more likely to be correct, even though the deduced reddening, $E_{B-V} = 0.31 \pm 0.04$, is significantly greater than the field reddening (Burstein and Heiles 1982). The UV nebular spectrum (in particular the weakness of both N V $\lambda 1240$ and O I $\lambda 1305$) is more reminiscent of RW Hya—a clear case of a hot stellar component—than of any of the main sequence accretors. This solution implies a ratio of hot to cool star radii $\log R_h/R_g = -2.69 \pm 0.09$, and a ratio of bolometric luminosities $\log L_h/L_g = -0.02 \pm 0.11$.

13. *RW Hydrae*.—Among the symbiotic systems we have examined, RW Hya appears to be the prototypical system containing a hot stellar component. Kafatos, Michalitsianos, and Hobbs (1980) favored a model with $\log T_h = 5.0$, and estimated a reddening of $E_{B-V} = 0.0013$ from the equivalent width of the interstellar Ly α absorption component. Our analysis of the subsequent UV observations by Slovak (1982), which differ insignificantly from those of Kafatos, Michalitsianos, and Hobbs in the strength or colors of the UV continuum, confirms this model: we find $\log T_h = 4.95 \pm 0.01$, $E_{B-V} = 0.014 \pm 0.019$, and deduce a ratio of stellar radii, $\log R_h/R_g = -2.94 \pm 0.05$, and bolometric luminosities, $\log L_h/L_g = -0.36 \pm 0.08$.

Yamamoto (1924) found a 370 day periodicity in the photographic light curve of RW Hya. By combining 18 epochs of maximum and 21 of minimum light tabulated by Gaposchkin (1954) with two epochs of spectroscopic conjunction (inferior conjunction of the hot component, which corresponds in phase to maximum light) from Merrill (1950), we derive the ephemeris,

$$\text{Max (pg)} = \text{JD } 2,421,519.2 (\pm 4.2) + 372.45 (\pm 0.30) \cdot E,$$

upon which the phases quoted in Table 4 are based. Minimum light falls at mean phase $\phi = 0.575 \pm 0.016$ in this ephemeris.

If we assume that this period is orbital in origin, the Roche lobe radius of the giant is $\sim 110 R_{\odot}$ for reasonable ($\sim 1 M_{\odot}$) masses for each of the two components. At the distance to RW Hya estimated by Kafatos, Michalitsianos, and Hobbs (1980), ~ 1.3 kpc, the M2 giant has a radius of $\sim 90 R_{\odot}$ and is thus nearly filling its tidal lobe. The periodic photometric variations in this system may then be due to a reflection effect, with the intense ultraviolet radiation of the hot component ($L_{\text{bol}} \approx 600 L_{\odot}$) heating the facing hemisphere of the cool giant. Similar orbital modulation is seen in AG Peg (Belyakina 1968), AG Dra (Meinunger 1979), and AX Per (Kenyon 1982).

14. *BX Monocerotis*.—This unique variable was excluded from Allen's (1979, 1982) catalogs of symbiotic stars because of the very low degree of excitation it displays optically. The ultraviolet spectrum obtained by Michalitsianos *et al.* (1982a) confirms the presence of a hot continuum source, upon which is superposed a weak emission line system, with C IV ($\lambda\lambda 1548, 1550$) the highest excitation species seen. Fe II and Mg II absorption blends are prominent in the near-ultraviolet, and Michalitsianos *et al.* note that these are typically seen in the spectra of early A and B type stars. Our C_1 index is likewise consistent with a stellar atmosphere of temperature $\log T = 3.956 \pm 0.002$, with a foreground reddening $E_{B-V} = 0.59 \pm 0.11$, but the C_2 index is significantly more negative than predicted by the Kurucz (1979) model atmospheres for such a star. Nevertheless, the deduced reddening is consistent with a distant object in the extinction map of Neckel and Klare (1980); BX Mon lies just outside their region 69, in which the reddening rises abruptly from $E_{B-V} = 0.25$ at 3.0 kpc to an asymptotic value $E_{B-V} = 0.65$ beyond 3.2 kpc. This would suggest an apparent distance modulus $(m - M)_V > 14.4$, and hence that the M star is of luminosity class Ib or brighter. Such a very bright M star is also indicated by the extraordinarily long period of the Mira-like optical light curve of this object:

$$\text{Max (pg)} = \text{JD } 2,430,345 + 1374 \cdot E$$

(Kukarkin *et al.* 1958; cf. Mayall 1940). This ephemeris is the basis of the phases quoted in Table 4.

15. *SY Muscae*.—SY Mus is one of a small number of symbiotic variables known to show a clear periodic component to its light curve (Uitterdijk 1934; Greenstein 1937; Bateson, Jones, and Menzies 1975; Kenyon 1983b). The observations in Table 4 are phased according to the ephemeris by Bateson, Jones, and Menzies:

$$\text{Min (} m_v \text{)} = \text{JD } 2,436,460 + 621.8 \cdot E.$$

The form of the light curve is reminiscent of the *U*-band light curve of AG Dra (Meinunger 1979; Oliverson and Anderson 1982b). No well-defined outburst of this variable has been recorded.

Michalitsianos *et al.* (1982a, b) noted a substantial increase in the strength of the UV continuum in the interval between their two *IUE* spectra. Since the first was obtained near phase 0.0, i.e., near visual minimum, they tentatively attributed the weakness of the continuum in that spectrum to an eclipse of the hot component by the cool giant. Although we can obtain a solution for the initial observation ($\log T_h = 3.952 \pm 0.003$, $E_{B-V} = -0.01 \pm 0.10$), the deduced reddening

is anomalously low for this low-latitude symbiotic star, and the deduced temperature of the hot component is far too low to account for the high excitation of the nebular emission line system superposed on the continuum. Rather, we are inclined to concur with the suggestion of Michalitsianos *et al.* (1982b) that the hot component was largely or possibly even totally eclipsed at the time of their first observation, and attribute the UV continuum largely to uneclipsed nebular emission. We have therefore listed only the solution to the second observation in Table 5.

The adopted solution for SY Mus implies a ratio of stellar radii, $\log R_h/R_g = -2.59 \pm 0.09$, and a ratio of bolometric luminosities, $\log L_h/L_g = 0.09 \pm 0.08$. SY Mus lies within field 147 in the galactic plane extinction map of Neckel and Klare (1980), which shows E_{B-V} rising abruptly from 0.0 at 0.2 kpc to a value of 0.4 in the interval from 0.4 to 1.7 kpc, then rising again to its asymptotic value, $E_{B-V} \approx 0.45$, at 2 kpc and beyond. Our deduced reddening is probably consistent, then, with any distance beyond 400 pc. The pronounced continuous orbital modulation of the light curve, both photographic (Uitterdijk 1934) and visual (Kenyon 1983b), suggests, however, that the cool component of SY Mus must be nearly lobe-filling, which would imply that the giant is a relatively luminous one and the system is thus rather distant. A lobe-filling giant would have a radius of $\sim 200 R_\odot$ and a bolometric luminosity $\sim 6000 L_\odot$ ($M_V \sim -3.2$), and imply a distance of 2.5 kpc.

16. *AR Pavonis*.—AR Pav was the first of the symbiotic stars to be clearly identified as an eclipsing binary (Mayall 1937). The hot component dominates much of the optical continuum, the eclipses being ~ 2 mag deep in the *UBV* bandpasses (Andrews 1974; Menzies *et al.* 1982). Optical spectroscopy through eclipse (Thackeray and Hutchings 1974) reveals a cF absorption line spectrum superposed on the hot star continuum, with the TiO absorption bands of the M3 giant companion visible only during eclipse. From the eclipse light curve, Thackeray and Hutchings (1974) estimate the radius of the hot component and giant as $R_h \sim 65 R_\odot$, $R_g \sim 135 R_\odot$, respectively; Andrews (1974) estimates $R_h \sim 45\text{--}75 R_\odot$, $R_g \sim 105 R_\odot$, on the assumption of a lobe-filling giant and an orbital inclination $i = 90^\circ$. These estimates of the giant's radius combined with its spectral type and *K* magnitude ($K = 7.16$ during eclipse, Glass and Webster 1973; the value quoted in Table 4 is that of the system out of eclipse) imply a distance of 4.5–5.8 kpc to AR Pav, placing it well out of the galactic plane, and giving an absolute magnitude for the giant $M_V = -1.5$ to -2.0 .

Within the (rather substantial) uncertainty in the level of the UV continuum of this object, we can obtain satisfactory fits for either a hot stellar companion or a main sequence accretor. The inferred hot stellar companion is, however, far too cool (~ 9500 K) to account for the high-excitation emission line system (including N v, C iv, Si iv, and He ii) seen in the spectra of this object, although at the same time somewhat hotter than indicated by the cF absorption spectrum. The implied ratio of radii for this solution, $\log R_h/R_g = -0.80 \pm 0.04$, is smaller, by a factor of 3 or more, than that deduced from the eclipse light curves. In fact, such a discrepancy points strongly towards a very flat, disklike geometry for the hot continuum source: the ratio of radii deduced from the strength of the UV continuum (in

comparison with the infrared *K* magnitude of the giant) is in effect a measure of the relative projected areas of each component, whereas the eclipse duration measures the extent of the hot component in the orbital plane. A factor of 3 discrepancy in these ratios thus implies a 9:1 flattening in the projected disk of the hot component. The conclusion that the hot component in AR Pav must be an accretion disk is further strengthened by the concentration, noted by Thackeray and Hutchings, of the He ii $\lambda 4686$ emitting region to the central region of the cF-type continuum source, and indeed Thackeray and Hutchings develop an accretion disk model for the hot component based on their optical spectroscopy and photometry. We stress that, as noted in § IIIb above, only the accretion disks around main sequence stars are capable of dominating the visual continuum of a late-type giant, as is clearly the case in AR Pav. The cF absorption spectrum is clearly typical of such a disk.

There remains some considerable uncertainty regarding the true foreground reddening to AR Pav. Andrews (1974) found $E_{B-V} < 0.1$ from observations of nearby field stars, an estimate which is in reasonable accord with the asymptotic reddening for this direction, $E_{B-V} = 0.10$, indicated by the Burstein and Heiles (1982) maps. Hutchings and Cowley (1982) estimated $E_{B-V} = 0.1$ as well from the depth of the 2200 Å feature in their eclipse observations, but both of our solutions give $E_{B-V} \approx 0.27$, in good agreement with the value ($E_{B-V} = 0.30$) determined by Slovak (1982) from the 2200 Å feature in the same spectrum we have analyzed. Thackeray and Hutchings (1974) found the diffuse interstellar absorption band at 4430 Å unusually strong, with a mean central intensity of $10 \pm 2\%$. This depth would imply $E_{B-V} = 0.94 \pm 0.19$ (Snedden *et al.* 1978), and Thackeray and Hutchings suggest that a major part of the absorption may arise in the circumstellar envelope, although they found no evidence for orbital modulation of the feature. Infrared observations of AR Pav extending to 3.5 μm show no evidence of circumstellar dust emission (Glass and Webster 1973), however, and the resolution of these differences remains problematic.

17. *AG Pegasi*.—AG Peg is one of the brightest symbiotic stars, and has been the subject of numerous optical studies. Gallagher *et al.* (1979) reviewed the history of this system in discussing their ultraviolet photometry from *OAO 2*. They found a bright stellar UV flux distribution, and noted the parallel between the spectroscopic and photometric evolution of AG Peg since its outburst (ca. 1855) and that of an extremely slow nova, arguing the case that this outburst is a thermonuclear event on a degenerate companion to the M giant. Keyes and Plavec (1979, 1980) undertook a thorough analysis of contemporaneous optical and ultraviolet spectrophotometry. They found that the continuum from 1200 Å to 5000 Å could be fitted by a 30,000 K Kurucz (1979) model atmosphere, with a ratio of hot to cool star radii $\log R_h/R_g = -2.02$, and bolometric luminosities $\log L_h/L_g = -0.35$. Such a star does not provide a significant flux of He ii ionizing photons, however, and they proposed a second, tentative model in which the near-ultraviolet continuum arises from nebular emission. This model contains a hot star of temperature 10^5 K, with relative radii $\log R_h/R_g = -2.65$ and relative bolometric luminosities $\log L_h/L_g = +0.46$.

The three *IUE* observations summarized in Table 4 show that the ultraviolet continuum of AG Peg varies significantly

within a time interval of 60 days or less. These observations are phased with respect to the photometric ephemeris of Meinunger (1981):

$$\text{Min}(B) = \text{JD } 2,428,250 + 827 \cdot E.$$

The corresponding UV colors are plotted for each observation in the C_1 - C_2 diagram in Figure 16.

Boyarchuk (1966*b*) classified the hot component optically as a WN6 star (indicative of a dense outflowing wind), and indeed AG Peg has been detected as a radio source with a spectral slope characteristic of free-free emission in an outflowing wind (Gregory, Kwok, and Seaquist 1977; Ghigo and Cohen 1981). The mass loss rate was estimated by Gregory, Kwok, and Seaquist as $\dot{M} = 3 \times 10^{-6}(d/\text{kpc})^2 M_{\odot} \text{ yr}^{-1}$, where d is the distance to AG Peg. We therefore suggest the UV variability of AG Peg arises from variations in an optically thick outflowing wind, rather than reflecting variations in a true stellar photosphere. This will tend to flatten the UV continuum (see the discussion of V1016 Cyg above), and displace the system toward positive C_1 and C_2 colors.

The formal solutions listed in Table 5 are based upon the mean UV colors ($m_{1300} - m_{1700}$, $m_{1700} - m_{2600}$, $m_{2200} - m_{2600}$) = $(-0.51 \pm 0.11, -0.92 \pm 0.10, -0.02 \pm 0.04)$; standard errors are quoted. All three solutions imply reddenings intermediate between the estimates of Gallagher *et al.* (1979), $E_{B-V} = 0.2$, and Keyes and Plavec (1980), $E_{B-V} = 0.12$. In the map of Burstein and Heiles (1982), an asymptotic interstellar reddening of $E_{B-V} = 0.07$ is indicated. (The infrared flux distribution of AG Peg shows no trace of an infrared excess [Glass and Webster 1973] which might signify circumstellar absorption.) The first solution with a hot star temperature of $\sim 23,500$ K is in reasonable agreement with the low-temperature solution of Keyes and Plavec (1979, 1980) (and also Boyarchuk 1966*b* and Gallagher *et al.* 1979), and implies a ratio of hot to cool star radii $\log R_h/R_g = -1.77 \pm 0.06$ and a ratio of bolometric luminosities $\log L_h/L_g = -0.35 \pm 0.07$. As noted above, such a low-temperature star cannot account for the high-excitation emission line system. This phenomenon is typical of Wolf-Rayet stars, and is evidently a manifestation of continuum formation in an expanding stellar atmosphere. The second solution, a disk-accreting white dwarf, is plausible only if the M giant is of luminosity class II or brighter (Gallagher *et al.* 1979; Keyes and Plavec 1980). Recent infrared spectrophotometry (Kenyon and Gallagher 1983) clearly points to a normal luminosity class III giant, however, which must then reside well within its Roche lobe. We therefore reject this solution as well, even though it is the only one of the three which predicts He II $\lambda 4686$ remotely comparable in strength with H β , as observed. In the third solution, the UV continuum at longer wavelengths is strongly affected by nebular emission. An electron temperature of 20,000 K is assumed, which is marginally higher than the 17,000 K temperature adopted by Boyarchuk (1966*b*). This solution implies ratios of stellar radii $\log R_h/R_g = -2.35 \pm 0.02$ and of bolometric luminosities $\log L_h/L_g = +0.04 \pm 0.11$. As with the low temperature solution, however, these conditions evidently refer to an extended photosphere formed in an outflowing wind; the temperature of the hot component is still insufficient to account for the strong high excitation nebular

lines if simple case B recombination applies (see § VI, below).

18. *RX Puppis*.—RX Pup belongs to that class of symbiotic stars, including R Aqr and V1016 Cyg discussed above, which show strong infrared excesses typical of hot circumstellar dust emission (Swings and Allen 1972; Glass and Webster 1973). As in the case of a number of other symbiotic stars with dust emission, RX Pup is also a radio source (Seaquist 1977; Wright and Allen 1978); although its rapid radio variability sets it apart from other symbiotic systems. Feast, Robertson, and Catchpole (1977) found strong infrared variability in RX Pup, similar to that in Mira variables. The identification of H₂O and CO absorption bands in the near-infrared by Barton, Phillips, and Allen (1979) confirms the presence of a late-type stellar component, although it remains undetected in optical spectra. Whitelock and Catchpole (1982; see also Whitelock *et al.* 1983*a*) found a well-defined period of 580 days in the 3.5 μm emission of RX Pup, and by combining their period with the 2.2 μm light curve observed by Feast, Robertson, and Catchpole (1977), we obtain the ephemeris:

$$\text{Max}(K) = \text{JD } 2,442,810 + 580 \cdot E,$$

upon which the phases quoted in Table 4 are calculated. The K magnitudes in Table 4 are interpolations of the light curve of Whitelock *et al.* (1983*b*).

During most of the past decade, RX Puppis showed only a relatively low-excitation optical emission line spectrum (Swings and Klutz 1976; Klutz, Simonetto, and Swings 1978; Klutz 1979). Klutz, Simonetto, and Swings considered the optical properties to be consistent with those of a heavily reddened late B or early A giant with an expanding envelope. Our solution to the mean colors of the two ultraviolet spectra we have analyzed is consistent with that suggestion, but by the time these spectra were obtained RX Pup had evolved into a much higher excitation phase, with the Balmer lines and Balmer continuum as strong emission features and the broad He II, N III, and [O III] lines similar to those found in WN7-8 stars (Klutz and Swings 1981). These features all point to a much hotter source than given by our solution, and, as in other dusty symbiotics, it is likely that our diagnostic colors have been distorted by anomalous reddening due to circumstellar dust. Nevertheless, the deduced reddening is in accord with the value, $E_{B-V} = 0.7$ -1.0, estimated by Klutz, Simonetto, and Swings from the strength of the interstellar Na I absorption lines, and the limit $E_{B-V} \geq 0.7$ derived from He II line ratios by Kafatos, Michalitsianos, and Feibelman (1982). RX Pup lies in region 100 of Neckel and Klare's (1980) extinction map, in which E_{B-V} reaches an asymptotic value of 0.6 at distances beyond 1 kpc.

While we have not obtained a viable solution for RX Pup, the two ultraviolet spectra, obtained near minimum and maximum of the infrared light curve, appear unaffected by the varying infrared emission (see Table 4; Fig. 16). This supports the attribution of the infrared variability to an underlying Mira variable.

19. *CL Scorpii*.—This rather low excitation symbiotic star lacks any detailed spectroscopic study. Payne-Gaposchkin (1957) suggested a 600 day periodicity in the long-term light curve compiled by Swope (1941). We find that available well-observed optical minima of this system can be represented

by the ephemeris:

$$\text{Min (pg)} = \text{JD } 2,427,020 (\pm 21) + 624.7 (\pm 1.5) \cdot E,$$

which was used to phase the UV observations in Table 4.

He II $\lambda 1640$ was very weak in the *IUE* spectrum obtained by Michalitsianos *et al.* (1982a), with N V absent and C IV of only modest strength. This low nebular excitation effectively precludes the hot star solution we obtained from the C_1 - C_2 continuum colors, and CL Sco therefore appears to be a main sequence accretor. Of the two such solutions we obtain, the first gives a clearly superior fit to the observed UV colors.

The continuum of CL Sco is very difficult to define at 2200 Å. The formal uncertainty in our deduced reddening, $E_{B-V} = 0.52 \pm 0.01$, is no doubt seriously underestimated, but all of our solutions give reddenings substantially higher than the $E_{B-V} = 0.1$ - 0.2 estimated by Michalitsianos *et al.* (1982a) from the same spectrum. No other direct estimate of the reddening to CL Sco has been made, but it lies just above region 228 in Neckel and Klare's (1980) study, in which the reddening appears constant, $E_{B-V} \approx 0.25$, out to distances of 2 kpc. However, the K5 spectral type assigned by Allen (1980, 1982) to the late-type component, combined with the observed $V-K \approx 5$, implies $E_{B-V} \geq 0.5$ (depending upon the contribution of the hot component at V).

If we take the period derived above as orbital in origin, then the late-type component must have a radius of $R_g \approx 140 R_\odot$ if it fills its Roche lobe and fuels a main sequence accretor (assuming a $1 M_\odot$ giant). The K5 giant should therefore be of luminosity class II, at a distance of 8 kpc. This would place CL Sco in the galactic bulge, roughly 1.1 kpc above the galactic plane, and imply that it is a member of the halo population (along with AG Dra and V443 Her). A determination of the systemic radial velocity of CL Sco could be instrumental in establishing the credibility of this model.

In the preceding pages, we have discussed possible models for each of the symbiotic stars in our sample. Five of these systems, Z And, CI Cyg, YY Her, AR Pav, and CL Sco, appear to contain main sequence stars accreting matter at $\sim 10^{-5} M_\odot \text{ yr}^{-1}$. The large derived accretion rates require the giants of these systems to fill their Roche lobes; this constraint is satisfied for CI Cyg, AR Pav, and perhaps Z And (Thackeray and Hutchings 1974; Kenyon and Gallagher 1983). The nature of the giant components in YY Her and CL Sco is uncertain: additional observations are needed to determine if these giants do indeed fill their tidal lobes. The remainder of our adopted solutions correspond to hot stellar sources with effective temperatures ranging from $\sim 10,000$ K up to $\sim 120,000$ K. No good candidates for white dwarf accretors were identified among the systems examined here. However, the hot stellar components in symbiotic systems could be accreting at rates low enough for the intrinsic hydrogen burning luminosity to dominate the accretion luminosity. Indeed, some accretion appears necessary to maintain the high observed temperatures, as noted by Tutukov and Yungel'son (1976, 1982) and by Paczyński and Rudak (1980). The giants in these systems are not required to fill their tidal lobes, although some (e.g., AG Dra) appear to do so.

Although we have shown that possible hot components for symbiotic systems can be differentiated on the basis of their UV continuum properties, these differences are also reflected

in their optical spectra. Those symbiotic stars identified as main sequence accretors all display [Ne v] and [Fe VII] emission at some time, while the hot stellar sources are of much lower excitation. Main sequence accretors typically undergo rapid "dwarf nova-like" outbursts; the outbursts of hot stellar sources, on the other hand, resemble more closely the slow classical novae in their spectroscopic and photometric behavior. We therefore tentatively group those S-type symbiotic stars displaying [Ne v] and [Fe VII] emission with main sequence accretors; the remaining S-type systems are more likely to be hot stellar sources.

VI. OBSERVATIONAL DIAGNOSTICS: THE EMISSION LINES

The emission line spectrum of a symbiotic star is very rich. This study has shown that the bright lines will be strong if either \dot{M} or T_h is large. In the main sequence accretors, the maximum temperature in the disk is $\sim 20,000$ K for $\dot{M} \sim 10^{-4} M_\odot \text{ yr}^{-1}$, while that of the boundary layer is $\sim 100,000$ K. Since these two sources have equal luminosities, essentially all nebular photons are produced by the boundary layer. For white dwarf accretors, both the disk and the boundary layer are copious sources of H and He ionizing photons, since $T_{\text{disk}} \sim 130,000$ K for $\dot{M} \sim 10^{-7} M_\odot \text{ yr}^{-1}$.

Optical spectrophotometric observations of several of the symbiotic stars discussed above were obtained by one of us (S. J. K.) on 1982 August 30–September 2 with the cooled, dual-beam intensified Reticon scanner (IRS) mounted on the white spectrograph of the KPNO No. 1 90 cm telescope. A wavelength range of 3500–6200 Å was secured using grating No. 26 with 600 lines mm^{-1} at a resolution of roughly 10 angstroms. These data were then calibrated on an absolute scale, and the absolute fluxes and equivalent widths of selected emission lines were extracted for comparison with the model solutions obtained above.

The observed equivalent widths of H γ and He II $\lambda 4686$ for five symbiotic stars with hot star solutions (cf. Table 5) are listed in Table 6, along with equivalent widths predicted by the models. The predicted equivalent widths are somewhat sensitive to the adopted spectral type of the giant, since the continuum flux shortward of 5000 Å decreases as the color temperature of the giant decreases. We have employed the

TABLE 6
COMPARISON OF MODEL AND OBSERVED EQUIVALENT WIDTHS:
HOT STELLAR SOURCES

SYSTEM	MODEL ^a	MODEL EQUIVALENT WIDTHS		OBSERVED EQUIVALENT WIDTHS	
		H γ	He II $\lambda 4686$	H γ	He II $\lambda 4686$
Z And	hs ₂	60	42	45	56
BF Cyg	hs ₁	38	0	42	7
AG Dra ^b	hs ₂	120	120	16	17
V443 Her	hs ₂	80	6	51	15
AG Peg	hs ₁	3	0	34	40
AG Peg	hs ₂	42	2	34	40

^a Model parameters are those appropriate to the corresponding solution in Table 5.

^b System at minimum.

TABLE 7
COMPARISON OF MODEL AND OBSERVED LINE FLUXES:
ACCRETING MAIN SEQUENCE STARS

SYSTEM	MODEL LINE FLUX ^a		OBSERVED LINE FLUX	
	H γ	He II $\lambda 4686$	H γ	He II $\lambda 4686$
Z And.....	1.4×10^{-11}	2.7×10^{-13}	1.1×10^{-11}	1.8×10^{-11}
CI Cyg.....	1.6×10^{-11}	1.5×10^{-12}	1.4×10^{-11}	2.6×10^{-11}
YY Her.....	5.2×10^{-13}	4.3×10^{-15}	1.4×10^{-13}	3.6×10^{-13}
V443 Her.....	4.7×10^{-12}	7.1×10^{-15}	6.4×10^{-12}	2.0×10^{-12}

^a Model parameters adopted from main sequence accretor (ms) solutions in Table 5; distances of 1.3 kpc (Z And), 2.1 kpc (CI Cyg), 5 kpc (YY Her), and 1.9 kpc (V443 Her) adopted from Kenyon (1983b).

spectral types given by Allen (1982); an uncertainty of ± 2 spectral subclasses represents a corresponding uncertainty of roughly $\pm 30\%$ in the predicted equivalent widths.

Equivalent widths are not appropriate measures of the emission line strengths for accreting systems, since the continuum is disk-dominated for $\lambda < 5000 \text{ \AA}$. The continuum level is thus a function of $\cos i$ (see eq. [6]), which is poorly known. We have therefore predicted the total line fluxes of H γ and $\lambda 4686$ for each accreting solution, and compare them with observations in Table 7. The observed fluxes have been corrected for interstellar reddening (Table 5), while the distances needed to derive predicted fluxes are from Kenyon (1983b) or Kenyon and Gallagher (1983). The estimated uncertainty in these predictions is $\pm 50\%$, and reflects the basic uncertainty in the distance estimates.

Given the uncertainties involved in the calculations and the fact that the observations of emission line fluxes are *not* simultaneous with the UV observations, the intensities of H γ (and other Balmer lines) agree remarkably well with the predictions. The situation is not so favorable when we consider $\lambda 4686$, since this line is grossly underpredicted for all models (except for the hot star solution to Z And). Willis and Wilson (1978) suggested that photoionization from the $n = 2$ level of He II is needed to correctly calculate Zanstra temperatures in the dense envelopes of Wolf-Rayet stars, and this mechanism may be important in some symbiotic stars as well. AG Peg has displayed Wolf-Rayet features for many years (Gallagher *et al.* 1979), and the observed He II $\lambda 1640$ equivalent width implies a Zanstra temperature of 30,000 K if this additional photoionization is included in the calculation. This is remarkably close to one of the solutions listed in Table 5, and a similar analysis correctly predicts the observed $\lambda 1640$ equivalent width of BF Cyg.

If the mechanism described above cannot be similarly applied to main sequence accretors, the overabundance of observed $\lambda 4686$ photons could be a serious blow to our models. CI Cygni is a well-studied example of this class which serves to illustrate the dilemma. As noted above, the star is an eclipsing binary with a period of 855.25 days, and the length of eclipse requires the giant to fill its Roche lobe (Hoffleit 1968; Kenyon *et al.* 1982). Kenyon and Gallagher (1983) analyzed this system in some detail, and derived a distance of 2.1 kpc. At this distance and extinction, the total He II $\lambda 4686$ flux (from a 2.1 m IIDS spectrum taken at KPNO by William Hartkopf) is $\sim 7.5 \times 10^{33} \text{ ergs s}^{-1}$. We may

rewrite equation (16) as:

$$N_{\gamma}(\text{He}^+) = (4\pi d^2 F_{4686}) \left(\frac{n_e n_{\text{He}^+}}{4\pi j_{4686}} \right) \alpha_{\text{He}}, \quad (23)$$

which gives $N_{\gamma}(\text{He}^+) \approx 9 \times 10^{45} \text{ photons s}^{-1}$ or $L(\text{He}^+) \approx 210 L_{\odot}$. From our measurement of the UV continuum color, the hot component in CI Cyg is accreting mass at $\sim 4 \times 10^{-5} M_{\odot} \text{ yr}^{-1}$, so the flux below 228 \AA implied by He II $\lambda 4686$ is about one-half the luminosity emitted by the boundary layer.

From this analysis, one might conclude that the boundary layer could provide the observed He II flux if it were at the proper temperature. For a blackbody boundary layer, the number of He⁺-ionizing photons is $N \propto R^2 T_{\text{BL}}^3 \exp(-1.4388/\lambda T_{\text{BL}})$, where $\lambda = 228 \text{ \AA}$, while $L_{\text{BL}} \propto R^2 T_{\text{BL}}^4$. Thus, $N T_{\text{BL}} \propto \exp(-1.4388/\lambda T_{\text{BL}})$ if L_{BL} is held constant. An increase in T_{BL} of only 30% would suffice to increase N by a factor of 5 for $\dot{M} \approx 4 \times 10^{-5} M_{\odot} \text{ yr}^{-1}$. As noted in our discussion of Figure 1, theoretical models of the temperature structure of the boundary layer are still extremely crude, so small changes in temperature are not impossible. However, it should be noted here that an increase in the boundary layer temperature introduces a problem with the hydrogen Balmer lines. For a constant boundary layer luminosity, the number of H-ionizing photons is roughly proportional to $1/T_{\text{BL}}$. Thus, an increase in this temperature actually *decreases* the number of hydrogen ionizing photons.

In point of fact, there are strong reasons for supposing that the blackbody approximation which we have adopted for our model boundary layers seriously overestimates the flux of hydrogen- and helium-ionizing photons (if $T_{\text{BL}} < 50,000 \text{ K}$ or $\log M < -5.5$; see § II above). The continua in model atmosphere calculations for hot stars (e.g., Osterbrock 1974; Kurucz 1979; Wesemael 1981) are greatly distorted by ionization edges on the blue side of the Planck peak. The larger opacity of the atmosphere to these ionizing photons tends to redistribute their flux to more transparent regions of the spectrum, sharply reducing the photoionization flux from the atmosphere. We therefore anticipate that more sophisticated treatments of the boundary layer continuum are likely to greatly exacerbate the situation in some systems.

The gross energetics of observed emission-line spectra demand that a large fraction ($\gtrsim \frac{1}{2}$) of the boundary layer luminosity from main sequence accretors be converted into recombination photons. For reasonable boundary layer flux distributions, however, the photoionization rate is at least a factor of 2-3 below that needed to reproduce the observed nebular flux, and the strength of higher excitation emission lines ($\sim 1 L_{\odot}$ in [Ne V] $\lambda 3426$ in CI Cyg) compounds this dilemma. Unless additional photoionization mechanisms can be identified (as in AG Peg, above), we are forced to conclude that *photoionization* cannot be the dominant ionization mechanism in the nebula of those symbiotic stars identified as main sequence accretors.

A promising alternative to photoionization is *mechanical* energy input into the nebula. For a solar-type accretor, the inner edge of the disk has a Keplerian velocity of $\sim 450 \text{ km s}^{-1}$, whereas the sound speed in the disk is $\sim 30 \text{ km s}^{-1}$. One may therefore anticipate the generation of highly supersonic shear turbulence in the boundary layer. In the presence of even a modest ambient magnetic field (~ 1 gauss), a substantial

fraction of the turbulent energy is converted into *hydromagnetic waves* (Alfvén 1947; Parker 1964). In the Sun, these hydromagnetic waves provide mechanical energy to the solar chromosphere and corona (Stein 1981), and it seems likely that they could energize an accretion disk corona as well (Galeev, Rosner, and Vaiana 1979). The extreme strength of [Ne v] and [Fe VII] in some symbiotic stars (Swings 1970) provides some support for this interpretation. Observations of these and other strong emission lines (e.g., the O III Bowen fluorescence lines) would be useful in measuring the input of mechanical energy into the nebula.

VII. THE OUTBURST

Finally, a word is in order regarding the outbursts of symbiotic stars. In an outburst, the spectrum changes from an M giant with a high excitation emission-line spectrum to an A-F supergiant with a shell-like emission spectrum of H I and He I (Belyakina 1979; Swings and Struve 1941; Merrill 1947). From our spectra, it appears that either the accretion model or the hot blackbody model can explain this change. We would require an increase in the accretion rate from $\sim 10^{-5} M_{\odot} \text{ yr}^{-1}$ to $\sim 10^{-3} M_{\odot} \text{ yr}^{-1}$ if the outbursts are accretion-powered events onto main sequence stars. For the hot blackbodies, we would need a large increase in the radius ($\Delta R/R \approx 100$) and luminosity ($\Delta L/L \approx 100$) to explain the changes in the spectrum. Such an event could be the result of a thermonuclear runaway in the hydrogen-burning shell of an accreting white dwarf (e.g., Tutukov and Yungel'son 1976; Paczyński and Rudak 1980; Iben 1982), or it could be due to a super-Eddington accretion event onto either a white dwarf or a main sequence star (e.g., Bath 1977). The behavior during the rise to light maximum, and during the decline from it, should be markedly different for these two types of events, and knowledge of the time-development of the UV and optical spectrum during outburst would be extremely useful in resolving this dilemma.

a) Thermonuclear Outbursts

In a thermonuclear outburst the rise to visual maximum is characterized by two phases: (i) a rapid increase in bolometric luminosity at nearly constant radius, followed by (ii) a slow expansion at constant bolometric luminosity (Paczynski and Żytkow 1978; Iben 1982; Kenyon and Truran 1983). On the basis of our synthetic spectra, we would anticipate that during phase (i) the nebular spectrum should grow dramatically in strength and excitation, but with relatively little disturbance to the continuum beyond the Balmer jump. A comparison of successive frames increasing in effective temperature in Figure 2 will serve to illustrate this phase. During the expansion phase (ii), the hot component evolves from a hot white dwarf ($R \sim 0.01 R_{\odot}$, $T_{\text{eff}} \sim 250,000 \text{ K}$) to an A-F supergiant ($R \sim 100 R_{\odot}$, $T_{\text{eff}} \sim 6000 \text{ K}$), if the envelope of the hot component has been accreted at a sufficiently slow rate ($\dot{M} < 10^{-8} M_{\odot} \text{ yr}^{-1}$). If the outburst has been preceded by a phase of more rapid mass accretion, however, this expansion is of a much smaller magnitude. Most of the optical brightening of the system occurs in this phase, with the nebular spectrum weakening substantially relative to the rapidly rising visible continuum. The higher-excitation nebular species disappear successively from the spectrum. Lower-excitation features decrease as well in equivalent width,

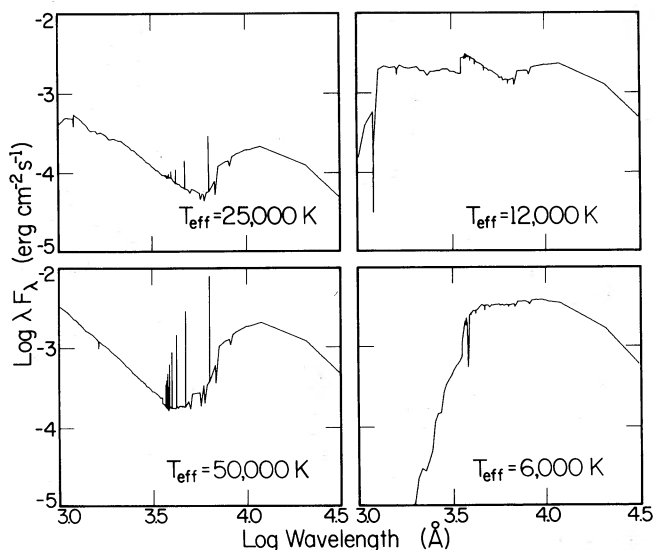


FIG. 17.—Synthetic spectra of a symbiotic star during a thermonuclear outburst. These spectra combine an M4 II giant with Kurucz (1979) model atmospheres with the indicated effective temperatures and luminosities of $10,000 L_{\odot}$.

although their absolute fluxes may at first increase. The spectroscopic development in phase (ii) may be visualized by comparing the 200,000 K panel of Figure 3 with successive frames decreasing in effective temperature in Figure 17.

The physical evolution of the underlying hot component in this model closely parallels that of slow classical novae (Paczynski and Żytkow 1978; Iben 1982; Kenyon and Truran 1983), but with one major difference from an observational standpoint: in classical novae, the vast increase in ultraviolet flux during phase (i) escapes unprocessed to infinity (except for potential thermal heating of the companion star) for lack of any significant circumsystem gas. Thus these objects display a nebular spectrum only *after* visual maximum, as their expanding photospheres turn optically thin. In symbiotic binaries, on the other hand, we would anticipate the pre-existence of a fairly dense ($n \sim 10^8 \text{ cm}^{-3}$) circumstellar envelope generated by the stellar wind of the giant companion. There is every reason to suppose then that the *rise* to maximum should be characterized by the appearance *first* of a nebular spectrum. In fact, however, phase (i) and phase (ii) may be so brief in duration (of the order of the rise time in a classical nova) as to stand little chance of optical detection before the system reaches late phase (ii).

In the decline from optical maximum, the hot component will retrace its evolution in the H-R diagram, as do the outbursting components in classical novae. During this phase novae typically possess dense outflowing winds, a circumstance which we may anticipate pertains to the hot components of these symbiotic stars as well. In novae, outflow velocities during decline are typically of the order of 10^3 km s^{-1} , i.e., much higher than typical wind velocities in normal late-type giants. If this holds true for thermonuclear symbiotic outbursts as well, the higher-excitation lines of the nebular spectrum as they reappear during optical decline should be substantially broader during decline than at minimum or during the rise to maximum.

The spectroscopic development of AG Peg since the optical maximum in 1850 has been discussed in some detail by Gallagher *et al.* (1979), and conforms closely to the sequence of events just described. We concur then with those authors in the opinion that the outburst of this symbiotic star is most readily understood in terms of a thermonuclear event on a white dwarf companion to the M3 giant.

b) Accretion Events

An accretion powered outburst is distinguished observationally from a thermonuclear event by an increase in the emitted flux at all wavelengths, rather than the flux redistribution which characterizes the rise to optical maximum (phase ii) and early optical decline in the thermonuclear case. During decline we again expect the systems qualitatively to retrace this evolution. The details of outburst development, however, depend critically upon the nature of the accreting object.

The outburst development for a white dwarf accretor can be visualized by following successively higher mass accretion rates in Figures 8 and 9, and reversing the sequence in the return to minimum. The most outstanding feature of this sequence is that, provided the accretion rate remains below the Eddington limit ($\sim 10^{-5} M_{\odot} \text{ yr}^{-1}$), the accretion disk is incapable of producing a substantial increase (more than a factor of ~ 2) in the continuum redward of the Balmer jump, nor does it ever develop the strong A-F continuum typical of symbiotic stars at maximum. Our models are incapable of producing outburst amplitudes greater than $\Delta V \approx 1$ mag at sub-Eddington accretion rates onto white dwarfs. The nebular spectrum increases uniformly in prominence, on the other hand, with rising accretion rate. Should the accretion rate exceed the Eddington limit, however, radiation pressure will disrupt the disk and lead to a rapid degradation of the emitted flux to the optical region, in a manner closely paralleling phase (ii) in the development of the thermonuclear outburst discussed above, and resulting in an A-F supergiant optical spectrum (Bath 1977).

Outburst development for a main sequence star accretor can be traced in Figures 7 and 10, again following sequences of increasing mass accretion rates. The flux distributions in this case are much softer than those of white dwarf accretors of equal bolometric luminosity. As a result, the disk continuum is capable of completely overwhelming that of the late-type giant, presenting the appearance of an F supergiant as \dot{M} nears $10^{-3} M_{\odot} \text{ yr}^{-1}$, well before radiation pressure (the Eddington limit) disrupts the disk. Our simple blackbody models of the boundary layer predict as well that the nebular emission increases both in excitation and in the equivalent widths of individual lines. Our predicted $H\beta$ equivalent width at maximum in this type of event ($\sim 56 \text{ \AA}$) is comparable to that observed in the 1973 outburst of CI Cyg (58.5 \AA ; Belyakina 1975). It must be stressed, however, that the behavior of the higher excitation lines depends crucially on the assumption that the nebula is photoionized. If mechanical heating is the dominant excitation mechanism near minimum, as discussed above, it is possible that increased accretion rates actually lead to less efficient nebular excitation, since the typical Mach number in the boundary layer flow decreases with increasing mass flux (the Keplerian velocity in the disk is unchanged—or perhaps even reduced if pressure support

of the disk becomes important—whereas the sound speed increases with the increased boundary layer temperature). The weakening or disappearance near maximum of the highest excitation features seen in CI Cyg lends some support to this idea.

VIII. SUMMARY

We have presented synthetic spectra for binaries consisting of a late-type giant and either: (1) a hot blackbody, (2) a white dwarf accretor, or (3) a main sequence accretor. Our results suggest that the UV color indices defined by equations (19) and (20) should be valuable tools for discriminating the nature of the hot components of symbiotic stars. In addition, these models predict correlations between the flux from recombination lines and physical parameters of the hot component. The available *IUE* and optical data have been used to test these models over a wide range of accretion rates and blackbody luminosities. We find that the properties of the continua of many symbiotic stars (e.g., CI Cyg and YY Her) can be understood if the hot components in these systems are main sequence stars accreting material at $\sim 10^{-5} M_{\odot} \text{ yr}^{-1}$. The Balmer line fluxes in this model underpredict the observed fluxes at quiescence by a factor of $\lesssim 2$. Other systems (e.g., BF Cyg, RW Hya, and AG Peg) seem to contain hot blackbodies ($R \lesssim 2 R_{\odot}$, $T_{\text{eff}} \gtrsim 25,000 \text{ K}$), as suggested by previous investigations. None of the models can explain the large flux from He II $\lambda 4686$ at quiescence. This problem can be removed for hot stellar sources if they have extended Wolf-Rayet like atmospheres (e.g., AG Peg). Main sequence accretors present a more serious dilemma: a slight increase in the boundary layer temperature could raise the $\lambda 4686$ flux, but it then cannot explain the strength of the Balmer lines. Our theoretical models imply that *photoionization* may not be the dominant ionization mechanism in the nebulae of those symbiotic stars that appear to contain main sequence accretors (e.g., CI Cyg and YY Her). We have suggested that *mechanical* energy input into the nebula via hydromagnetic waves produced in the boundary layer is a promising ionization mechanism for these nebulae. Finally, we have shown that the optical spectrum of a symbiotic star in outburst may be produced by either (i) a blackbody at $T_{\text{eff}} \approx 6000\text{--}10,000 \text{ K}$, (ii) a white dwarf accreting matter at a rate *above* the Eddington limit ($\dot{M} \gtrsim 10^{-5} M_{\odot} \text{ yr}^{-1}$), or (iii) a main sequence star accreting matter near the Eddington limit ($\dot{M} \sim 10^{-3} M_{\odot} \text{ yr}^{-1}$). We have described the evolution of the outburst for each of these possibilities, and have identified the critical stages when UV and optical spectra should be obtained.

The authors would like to thank J. W. Truran, J. S. Gallagher, T. Mouschovias, F. Wesemael, and R. E. Williams for encouragement and comments during the course of this work. Special thanks are extended to Bob MacFarlane, Sue Killian, and Sue Sprandel for a masterful job at drafting the figures. We would also like to thank Deidre Hunter, William Hartkopf, David Lien, Chris Anderson, Andy Michalitsianos, and Bob Stencel for providing us with the optical and UV data and the data programs needed to complete this project. We also thank J. A. Mattei of the AAVSO and F. M. Bateson of the RASNZ for providing

visual magnitudes of the individual symbiotics examined in this paper. Lastly, and most especially, we thank Mirek Plavec, whose numerous constructive criticisms of the original version of this paper led, we believe, to substantial improvements in our approach to this problem. An early version of

this work was presented at the North American Workshop on Symbiotic Stars and Santa Cruz Summer Workshop on Cataclysmic Variables. We would like to thank the organizers of these workshops for providing the stimulating environment which encouraged the completion of this work.

REFERENCES

- Ahern, F. J., FitzGerald, M. P., Marsh, K. A., and Purton, C. R. 1977, *Astr. Ap.*, **58**, 35.
- Alfvén, H. 1947, *Ark. Mat. Astr. Fys.*, **29B**, No. 2.
- Allen, C. W. 1973, *Astrophysical Quantities* (3d ed.; London: Athlone).
- Allen, D. A. 1979, in *IAU Colloquium 46, Changing Trends in Variable Star Research*, ed. F. M. Bateson, J. Smak, and I. H. Urch (Hamilton, N.Z.: University of Waikato), p. 125.
- . 1980, *M.N.R.A.S.*, **192**, 521.
- . 1981, *M.N.R.A.S.*, **197**, 739 [Erratum: 1982, *M.N.R.A.S.*, **201**, 1199].
- . 1982, in *IAU Colloquium 70, The Nature of Symbiotic Stars*, ed. M. Freidjung and R. Viotti (Dordrecht: Reidel), p. 27.
- Aller, L. H. 1954, *Pub. DAO Victoria*, **9**, 321.
- Altamore, A., Baratta, G. B., Cassatella, A., Friedjung, M., Giangrande, A., and Viotti, R. 1981, *Ap. J.*, **245**, 630.
- Altamore, A., Baratta, G. B., Cassatella, A., Giangrande, A., Ponz, D., Ricciardi, O., and Viotti, R. 1982, in *IAU Colloquium 70, The Nature of Symbiotic Stars*, ed. M. Freidjung and R. Viotti (Dordrecht: Reidel), p. 183.
- Anderson, C. M., Cassinelli, J. P., Oliverson, N. A., Myers, R. V., and Sanders, W. T. 1982, in *IAU Colloquium 70, The Nature of Symbiotic Stars*, ed. M. Freidjung and R. Viotti (Dordrecht: Reidel), p. 117.
- Anderson, C. M., Cassinelli, J. P., and Sanders, W. T. 1981, *Ap. J. (Letters)*, **257**, L127.
- Andrews, P. J. 1974, *M.N.R.A.S.*, **167**, 635.
- Andrillat, Y., Ciatti, F., and Swings, J. P. 1982, *Ap. Space Sci.*, **83**, 423.
- Baade, W. 1943, *Ann. Rept. Dir. Mt. Wilson Obs. 1943-1944*, p. 12.
- Bailey, J. E. 1975, *J. Brit. Astr. Assoc.*, **85**, 217.
- Barton, J. R., Phillips, B. A., and Allen, D. A. 1979, *M.N.R.A.S.*, **187**, 813.
- Bateson, F. M., Jones, A. F., and Menzies, B. 1975, *Pub. Variable Star Section Roy. Astr. Soc. New Zealand*, No. 3, p. 40.
- Bath, G. T. 1977, *M.N.R.A.S.*, **178**, 203.
- Bath, G. T., and Pringle, J. E. 1982, *M.N.R.A.S.*, **201**, 345.
- Belyakina, T. S. 1968, *Astr. Zh.*, **45**, 139 (English transl. *Soviet Astr.—AJ*, **12**, 110).
- . 1975, in *IAU Symposium 67, Variable Stars and Stellar Evolution*, ed. V. E. Sherwood and L. Plaut (Dordrecht: Reidel), p. 397.
- . 1979, *Izv. Krymsk. Astrofiz. Obs.*, **59**, 133 (English transl. 1980, *Bull. Crimean Ap. Obs.*, **59**, 98).
- Benvenuti, O., and Perinotto, M. 1981, *Astr. Ap.*, **95**, 127.
- Berman, L. 1932, *Pub. A.S.P.*, **44**, 318.
- Bidelman, W. P. 1954, *Ap. J. Suppl.*, **1**, 175.
- Bloch, M., and Tchong, M.-L. 1951, *Ann. d'Ap.*, **14**, 266.
- Boyarchuk, A. A. 1966a, *Astrofizika*, **2**, 101 (English transl. 1967, *Astrophysics*, **2**, 50).
- . 1966b, *Astr. Zh.*, **43**, 976 (English transl. *Soviet Astr.—AJ*, **10**, 783).
- . 1967, *Astr. Zh.*, **44**, 1016 (English transl. *Soviet Astr.—AJ*, **11**, 818).
- . 1969, *Izv. Krymsk. Astrofiz. Obs.*, **39**, 124.
- Brocklehurst, M. 1971, *M.N.R.A.S.*, **153**, 471.
- Brown, R. L., and Mathews, W. G. 1970, *Ap. J.*, **160**, 939.
- Burstein, D., and Heiles, C. 1982, *A.J.*, **87**, 1165.
- Cassatella, A., Patriarchi, P., Selvelli, P. L., Bianchi, L., Cacciari, C., Heck, A., Perryman, M., and Wamsteker, W. 1982, in *Third European IUE Conference*, ed. E. Rolfe, A. Heck, and B. Battrick (ESA SP-176), p. 229.
- Cassinelli, J. P. 1971, *Ap. J.*, **165**, 265.
- Catchpole, R. M., Robertson, B. S. C., Lloyd-Evans, T. H. H., Feast, M. W., Glass, I. S., and Carter, B. S. 1979, *S. Africa Astr. Obs. Circ.*, **1**, 61.
- Cester, B. 1968, *Inf. Bull. Var. Stars*, No. 291.
- Cohen, M., and Barlow, M. J. 1974, *Ap. J.*, **193**, 401.
- Córdova, F. A., Mason, K. O., and Nelson, J. E. 1981, *Ap. J.*, **245**, 609.
- Cox, D. P., and Mathews, W. G. 1969, *Ap. J.*, **155**, 859.
- Drake, S. A., and Ulrich, R. K. 1981, *Ap. J.*, **248**, 380.
- Edgen, O. J. 1964, *R. Obs. Bull.*, No. 84.
- Eiroa, C., Hefele, H., and Qian, Z.-U. 1982, in *IAU Colloquium 70, The Nature of Symbiotic Stars*, ed. M. Freidjung and R. Viotti (Dordrecht: Reidel), p. 43.
- Feast, M. W., Robertson, B. S. C., and Catchpole, R. M. 1977, *M.N.R.A.S.*, **179**, 499.
- Feibelman, W. A. 1982, *Ap. J.*, **258**, 562.
- Fernie, J. D., and Brooker, A. A. 1961, *Ap. J.*, **133**, 1088.
- Fried, J. W. 1980, *Astr. Ap.*, **88**, 141.
- Frogel, J. A., Persson, S. E., and Cohen, J. G. 1981, *Ap. J.*, **246**, 842.
- Galeev, A. A., Rosner, R., and Vaiana, G. S. 1979, *Ap. J.*, **229**, 318.
- Gallagher, J. S., Holm, A. V., Anderson, C. M., and Webbink, R. F. 1979, *Ap. J.*, **229**, 994.
- Gaposchkin, S. 1954, *Ann. Harvard Obs.*, **115**, 899.
- Ghigo, F. D., and Cohen, N. L. 1981, *Ap. J.*, **245**, 988.
- Gillett, F. C., Merrill, K. M., and Stein, W. A. 1971, *Ap. J.*, **164**, 83.
- . 1972, *Ap. J.*, **172**, 367.
- Glass, I. S., and Webster, B. L. 1973, *M.N.R.A.S.*, **165**, 77.
- Greenstein, N. 1937, *Bull. Harvard Coll. Obs.*, No. 906, p. 3.
- Gregory, P. C., Kwok, S., and Seaquist, E. R. 1977, *Ap. J.*, **211**, 429.
- Hack, M. 1979, *Nature*, **279**, 305.
- Hack, M., Persic, M., and Selvelli, P. L. 1982, in *Third European IUE Conference*, ed. E. Rolfe, A. Heck, and B. Battrick (ESA SP-176), p. 193.
- Hack, M., and Selvelli, P. L. 1982a, *Astr. Ap.*, **107**, 200.
- . 1982b, in *IAU Colloquium 70, The Nature of Symbiotic Stars*, ed. M. Freidjung and R. Viotti (Dordrecht: Reidel), p. 131.
- Harkness, R. P. 1979, in *IAU Colloquium 53, White Dwarfs and Variable Degenerate Stars*, ed. H. M. Van Horn and V. Weidemann (Rochester: University of Rochester), p. 464.
- Harvey, P. M. 1974, *Ap. J.*, **188**, 95.
- Herbig, G. H. 1950, *Pub. A.S.P.*, **62**, 211.
- Herter, T., Lacasse, M. G., Wesemael, F., and Winget, D. E. 1979, *Ap. J. Suppl.*, **39**, 513.
- Hjellming, R. M., and Bignell, R. C. 1982, *Science*, **216**, 1279.
- Hoffleit, D. 1968, *Irish Astr. J.*, **8**, 149.
- Hogg, F. S. 1934, *Pub. A.A.S.*, **8**, 14.
- Hummer, D. G., and Mihalas, D. 1970, *M.N.R.A.S.*, **147**, 339.
- Huang, C.-C. 1982, in *IAU Colloquium 70, The Nature of Symbiotic Stars*, ed. M. Freidjung and R. Viotti (Dordrecht: Reidel), p. 185.
- Hutchings, J. B., and Cowley, A. P. 1982, *Pub. A.S.P.*, **94**, 107.
- Ianna, P. A. 1964, *Ap. J.*, **139**, 780.
- Iben, I., Jr. 1982, *Ap. J.*, **259**, 244.
- Iijima, T. 1982, *Astr. Ap.*, **116**, 210.
- Jenkins, L. F. 1952, *General Catalogue of Trigonometric Stellar Parallaxes* (New Haven: Yale Univ. Obs.), p. 20.
- Johnson, H. L. 1965, *Ap. J.*, **141**, 923.
- . 1966, *Ann. Rev. Astr. Ap.*, **4**, 193.
- Johnson, H. M. 1980, *Ap. J.*, **237**, 840.
- . 1982, *Ap. J.*, **253**, 224.
- Joy, A. H. 1926, *Ap. J.*, **63**, 281.
- Kafatos, M., Michalitsianos, A. G., and Feibelman, W. A. 1982, *Ap. J.*, **257**, 204.
- Kafatos, M., Michalitsianos, A. G., and Hobbs, R. W. 1980, *Ap. J.*, **240**, 114.
- Kaler, J. B. 1976, *Ap. J.*, **210**, 843.
- . 1980, *IAU Circ.*, No. 3540.
- . 1981, *Ap. J.*, **245**, 568.
- . 1983, private communication.
- Karzas, W. J., and Latter, R. 1961, *Ap. J. Suppl.*, **6**, 167.
- Kenyon, S. J. 1982, *Pub. A.S.P.*, **94**, 165.
- . 1983a, in *Cataclysmic Variables and Low Mass X-ray Binaries*, ed. D. Q. Lamb and J. Patterson (Dordrecht: Reidel), in press.
- . 1983b, Ph.D. thesis, University of Illinois.
- Kenyon, S. J., and Gallagher, J. S. 1983, *A.J.*, **88**, 666.
- Kenyon, S. J., and Truran, J. W. 1983, *Ap. J.*, **273**, 280.
- Kenyon, S. J., Webbink, R. F., Gallagher, J. S., and Truran, J. W. 1982, *Astr. Ap.*, **106**, 109.
- Keyes, C. D., and Plavec, M. J. 1979, in *The Universe at Ultraviolet Wavelengths*, ed. R. D. Chapman (NASA CP-2171), p. 443.
- . 1980, in *IAU Symposium 88, Close Binary Stars: Observations and Interpretation*, ed. M. J. Plavec, D. M. Popper, and R. K. Ulrich (Dordrecht: Reidel), p. 365.
- Klutz, M. 1979, *Astr. Ap.*, **73**, 244.
- Klutz, M., Simonetto, O., and Swings, J. P. 1978, *Astr. Ap.*, **66**, 283.
- Klutz, M., and Swings, J. P. 1981, *Astr. Ap.*, **96**, 406.
- Knacke, R. F. 1972, *Ap. Letters*, **11**, 201.
- Kraft, R. P. 1958, *Ap. J.*, **127**, 625.
- Krautter, J., Klare, G., Wolf, B., Duerback, H. W., Rahe, J., Vogt, N., and Wargon, W. 1981, *Astr. Ap.*, **102**, 337.
- Kuiper, G. P. 1940, *Pub. A. A. S.*, **10**, 57.
- Kukarkin, B. V., Parenago, P. P., Efremov, Yu. I., and Kholopov, P. N. 1958, *General Catalogue of Variable Stars* (2d ed.; Moscow: Akad. Nauk S.S.S.R.).
- Kurucz, R. L. 1979, *Ap. J. Suppl.*, **40**, 1.

- Kwok, S. 1982, in *IAU Colloquium 70, The Nature of Symbiotic Stars*, ed. M. Freidjung and R. Viotti (Dordrecht: Reidel), p. 17.
- Lawrence, G. M., Ostriker, J. P., and Hesser, J. E. 1967, *Ap. J. (Letters)*, **148**, L161.
- Lee, T. A. 1970, *Ap. J.*, **162**, 217.
- Lynden-Bell, D., and Pringle, J. E. 1974, *M.N.R.A.S.*, **168**, 603.
- MacFarlane, M. J. 1979, *Univ. Texas, Publ. Astr.*, No. 15.
- Mammano, A., and Chincarini, G. 1966, *Mem. Soc. Astr. Ital.*, **37**, 421.
- Mammano, A., and Ciatti, F. 1975, *Astr. Ap.*, **39**, 405.
- Mammano, A., and Taffara, S. 1978, *Astr. Ap. Suppl.*, **34**, 211.
- Mattei, J. A. 1982, private communication.
- Mayall, M. W. 1937, *Ann. Harvard Obs.*, **105**, 491.
- . 1940, *Harvard Obs. Bull.*, No. 913, p. 8.
- Mayo, S. K., Wickramasinghe, D. T., and Whelan, J. A. J. 1980, *M.N.R.A.S.*, **193**, 793.
- McLaughlin, D. B. 1960, in *Stellar Atmospheres*, ed. J. L. Greenstein (Chicago: University of Chicago Press), p. 585.
- Meinunger, L. 1979, *Inf. Bull. Var. Stars*, No. 1611.
- . 1981, *Inf. Bull. Var. Stars*, No. 2016.
- Menzies, J. W., Coulson, I. M., Caldwell, J. A. R., and Corben, P. M. 1982, *M.N.R.A.S.*, **200**, 463.
- Merlin, P. 1972, *Comptes Rendus*, **275**, 45.
- . 1973, *Astr. Ap.*, **23**, 363.
- Merrill, P. W. 1921, *Ap. J.*, **53**, 375.
- . 1940, *Spectra of Long Period Variable Stars* (Chicago: University of Chicago).
- . 1947, *Ap. J.*, **105**, 120.
- . 1950, *Ap. J.*, **111**, 484.
- Merrill, P. W., and Burwell, C. G. 1950, *Ap. J.*, **112**, 72.
- Meyer, D. M., and Savage, B. D. 1981, *Ap. J.*, **248**, 545.
- Michalitsianos, A. G., and Kafatos, M. 1982, *Ap. J. (Letters)*, **262**, L47.
- Michalitsianos, A. G., Kafatos, M., and Hobbs, R. W. 1980, *Ap. J.*, **237**, 506.
- Michalitsianos, A. G., Kafatos, M., Feibelman, W. A., and Hobbs, R. W. 1982a, *Ap. J.*, **253**, 735.
- Michalitsianos, A. G., Kafatos, M., Feibelman, W. A., and Wallerstein, G. 1982b, *Astr. Ap.*, **109**, 136.
- Mikolajewska, J., and Mikolajewski, M. 1980, *Acta Astr.*, **30**, 347.
- Morrison, D., and Simon, T. 1973, *Ap. J.*, **186**, 193.
- Nassau, J. J., and Cameron, D. M. 1954, *Ap. J.*, **119**, 75.
- Neckel, T., and Klare, G. 1980, *Astr. Ap. Suppl.*, **42**, 251.
- Newell, R. T., and Hjellming, R. M. 1981, in *Proceedings of the North American Workshop on Symbiotic Stars*, ed. R. E. Stencel (Boulder: JILA), p. 16.
- Nomoto, K., Nariai, K., and Sugimoto, D. 1979, *Pub. Astr. Soc. Japan*, **31**, 257.
- Nussbaumer, H., and Schild, H. 1981, *Astr. Ap.*, **101**, 118.
- O'Connell, R. W. 1973, *A.J.*, **78**, 1074.
- Oliversen, N. G., Anderson, C. M., Cassinelli, J. P., Sanders, W. T., and Kaler, J. B. 1980, *Bull. AAS*, **12**, 819.
- Oliversen, N. G., and Anderson, C. M. 1982a, in *IAU Colloquium 70, The Nature of Symbiotic Stars*, ed. M. Freidjung and R. Viotti (Dordrecht: Reidel), p. 71.
- . 1982b, in *IAU Colloquium 70, The Nature of Symbiotic Stars*, ed. M. Freidjung and R. Viotti (Dordrecht: Reidel), p. 177.
- Osterbrock, D. E. 1974, *Astrophysics of Gaseous Nebulae* (San Francisco: Freeman).
- Paczyński, B. 1965, *Acta Astr.*, **15**, 197.
- Paczyński, B., and Rudak, B. 1980, *Astr. Ap.*, **82**, 349.
- Paczyński, B., and Żytkow, A. N. 1978, *Ap. J.*, **222**, 604.
- Pagel, B. E. J. 1958, *Mem. Soc. Roy. Sci. Liège*, 4th Ser., **20**, 177.
- Parker, E. N. 1964, *Ap. J.*, **140**, 1170.
- Payne-Gaposchkin, C. 1946, *Ap. J.*, **104**, 362.
- . 1952, *Ann. Harvard Obs.*, **115**, 121.
- . 1954, *Ann. Harvard Obs.*, **113**, 189.
- . 1957, *The Galactic Novae* (Amsterdam: North Holland), p. 225.
- Perinotto, M., and Benvenuti, P. 1981a, *Astr. Ap.*, **100**, 241.
- . 1981b, *Astr. Ap.*, **101**, 88.
- Plavec, M. J. 1982, in *IAU Colloquium 70, The Nature of Symbiotic Stars*, ed. M. Freidjung and R. Viotti (Dordrecht: Reidel), p. 231.
- Pringle, J. E. 1977, *M.N.R.A.S.*, **178**, 195.
- Pringle, J. E., and Savonije, G. J. 1979, *M.N.R.A.S.*, **187**, 777.
- Pucinskas, A. 1970, *Bull. Vilnius Univ. Astr. Obs.*, No. 27, p. 24.
- Puetter, R. C., Russell, R. W., Soifer, B. T., and Willner, S. P. 1978, *Ap. J. (Letters)*, **223**, L93.
- Purton, C. R., Feldman, P. A., and Marsh, K. A. 1973, *Nature Phys. Sci.*, **245**, 5.
- Ridsdal, S., and Weigert, A. 1971, *Astr. Ap.*, **13**, 367.
- Ridgway, S. T., Joyce, R. R., White, N. M., and Wing, R. F. 1980, *Ap. J.*, **235**, 126.
- Ritter, H. 1982, *Catalogue of Cataclysmic Binaries, Low Mass X-Ray Binaries and Related Objects* (Munich: MPI f. Phys. Ap.).
- Roman, N. G. 1953, *Ap. J.*, **117**, 467.
- Sahade, J., Brandi, E., and Fontenla, J. M. 1981, *Rev. Mexicana Astr. Ap.*, **6**, 201.
- Sanduleak, N., and Stephenson, C. B. 1973, *Ap. J.*, **185**, 899.
- Savage, B. D., and Mathis, J. S. 1979, *Ann. Rev. Astr. Ap.*, **17**, 73.
- Seaquist, E. R. 1977, *Ap. J.*, **211**, 547.
- Seaquist, E. R., and Gregory, P. C. 1973, *Nature Phys. Sci.*, **245**, 85.
- Seaton, M. J. 1960, *Rept. Prog. Phys.*, **23**, 313.
- . 1979, *M.N.R.A.S.*, **187**, 73P.
- Shakura, N. I., and Sunyaev, R. A. 1973, *Astr. Ap.*, **24**, 337.
- Slovak, M. H. 1980, *Bull. AAS*, **12**, 868.
- . 1982, Ph.D. thesis, University of Texas.
- Slovak, M. H., and Africano, J. 1978, *M.N.R.A.S.*, **185**, 591.
- Snedden, C., Gehr, R. D., Hackwell, J. A., York, D. G., and Snow, T. P. 1978, *Ap. J.*, **223**, 168.
- Spitzer, L., and Greenstein, J. L. 1951, *Ap. J.*, **114**, 407.
- Stein, R. F. 1981, *Ap. J.*, **246**, 966.
- Stencel, R. E. 1982, private communication.
- Stencel, R. E., Michalitsianos, A. G., Kafatos, M., and Boyarchuk, A. A. 1982, *Ap. J. (Letters)*, **253**, L77.
- Stephens, J. R. 1980, *Ap. J.*, **237**, 450.
- Swings, J. P., and Allen, D. A. 1972, *Pub. A.S.P.*, **84**, 523.
- Swings, J. P., and Klutz, M. 1976, *Astr. Ap.*, **46**, 303.
- Swings, P. 1970, in *Spectroscopic Astrophysics*, ed. G. Herbig (Berkeley: University of California), p. 189.
- Swings, P., and Struve, O. 1941, *Ap. J.*, **93**, 356.
- Swope, H. H. 1941, *Ap. J.*, **94**, 140.
- Taranova, O. G., and Yudin, B. F. 1980, *Pis'ma Astr. Zh.*, **6**, 495 (English transl. 1981, *Soviet Astr. Letters*, **6**, 273).
- . 1981, *Astr. Zh.*, **58**, 1249 (English transl. 1981, *Soviet Astr.—AJ*, **25**, 710).
- Thackeray, A. D., and Hutchings, J. B. 1974, *M.N.R.A.S.*, **167**, 319.
- Tift, W. G., and Greenstein, J. L. 1958, *Ap. J.*, **127**, 160.
- Tutukov, A. V., and Yungel'son, L. R. 1976, *Astrofizika*, **12**, 521 (English transl. 1977, *Astrophysics*, **12**, 342).
- . 1982, in *IAU Colloquium 70, The Nature of Symbiotic Stars*, ed. M. Freidjung and R. Viotti (Dordrecht: Reidel), p. 283.
- Tylenda, R. 1977, *Acta Astr.*, **27**, 3.
- . 1982, *Acta Astr.*, **31**, 127.
- Uitterdijk, J. 1934, *Bull. Astr. Inst. Netherlands*, **7**, 177.
- Viotti, R., Giangrande, A., Ricciardi, O., and Cassatella, A. 1982, in *IAU Colloquium 70, The Nature of Symbiotic Stars*, ed. M. Freidjung and R. Viotti (Dordrecht: Reidel), p. 125.
- Walker, M. F. 1957, in *IAU Symposium 3, Non-Stable Stars*, ed. G. Herbig (London: Cambridge University), p. 46.
- Wallerstein, G. 1968, *Observatory*, **88**, 111.
- . 1981, *Observatory*, **101**, 172.
- . 1983, *Pub. A.S.P.*, **95**, 135.
- Wallerstein, G., and Greenstein, J. L. 1980, *Pub. A.S.P.*, **92**, 275.
- Warner, B. 1972, *M.N.R.A.S.*, **159**, 95.
- Webbink, R. F. 1975, *M.N.R.A.S.*, **171**, 555.
- . 1976, *Nature*, **262**, 271.
- . 1979, in *IAU Colloquium 46, Changing Trends in Variable Star Research*, ed. F. M. Bateson, J. Smak, and I. H. Urch (Hamilton, N.Z.: University of Waikato), p. 102.
- . 1981, in *Proceedings of the North American Workshop on Symbiotic Stars*, ed. R. E. Stencel (Boulder: JILA), p. 19.
- Webbink, R. F., and Kenyon, S. J. 1984, in preparation.
- Webster, B. L., and Allen, D. A. 1975, *M.N.R.A.S.*, **171**, 171.
- Wesemael, F. 1981, *Ap. J. Suppl.*, **45**, 177.
- Wesemael, F., Auer, L. H., Van Horn, H. M., and Savedoff, M. P. 1980, *Ap. J. Suppl.*, **43**, 159.
- Whitelock, P. A., and Catchpole, R. M. 1982, in *IAU Colloquium 70, The Nature of Symbiotic Stars*, ed. M. Freidjung and R. Viotti (Dordrecht: Reidel), p. 207.
- Whitelock, P. A., Catchpole, R. M., Feast, M. W., Roberts, G., and Carter, B. S. 1983a, *M.N.R.A.S.*, **203**, 363.
- Whitelock, P. A., Feast, M. W., Catchpole, R. M., Carter, B. S., and Roberts, G. 1983b, *M.N.R.A.S.*, **203**, 351.
- Williams, R. E. 1980, *Ap. J.*, **235**, 939.
- Willis, A. J., and Wilson, R. 1978, *M.N.R.A.S.*, **182**, 589.
- Willson, L. A., Garnavich, P., and Mattei, J. A. 1981, *Inf. Bull. Var. Stars*, No. 1961.
- Wilson, R. E. 1942, *Ap. J.*, **96**, 371.
- Wing, R. F., and Carpenter, K. G. 1979, in *The Universe at Ultraviolet Wavelengths*, ed. R. D. Chapman (NASA CP-2171), p. 341.
- Woolf, N. J. 1973, *Ap. J.*, **185**, 229.
- Wright, A. E., and Allen, D. A. 1978, *M.N.R.A.S.*, **184**, 893.
- Wright, A. E., and Barlow, M. J. 1975, *M.N.R.A.S.*, **170**, 41.
- Wu, C.-C., Faber, S. M., Gallagher, J. S., Peck, M., and Tinsley, B. M. 1980, *Ap. J.*, **237**, 290.
- Yamamoto, I. 1924, *Harvard Obs. Bull.*, No. 810, p. 4.
- Yamashita, Y., and Maehara, H. 1979, *Pub. Astr. Soc. Japan*, **31**, 307.
- Yudin, B. F. 1982, *Astr. Zh.*, **59**, 307 (English transl. *Soviet Astr.—AJ*, **26**, 187).

S. J. KENYON: Center for Astrophysics, 60 Garden Street, Cambridge, MA 02138

R. F. WEBBINK: Department of Astronomy, University of Illinois, 1011 W. Springfield Avenue, Urbana, IL 61801-3000